

1 **Fluids associated with hydrothermal dolomitization in St.**
2 **George Group, western Newfoundland, Canada**

3

4 *James Conliffe¹, Karem Azmy¹, Sarah A. Gleeson² and Denis Lavoie³*

5

6 ¹ *Department of Earth Sciences, Memorial University of Newfoundland, St John's, NL*
7 *A1B 3X5, Canada*

8 ² *Department of Earth and Atmospheric Sciences, University of Alberta, Edmonton,*
9 *Alberta, Canada T6G 2E3*

10 ³ *Geological Survey of Canada, GSC-Q, Natural Resources Canada, 490 de la*
11 *Couronne, Québec, Qc, G1K 9A9.*

12

13 ***Running title: Hydrothermal dolomite in western Newfoundland***

14

15 ***Corresponding author:***

16 *E-mail address: jamesconliffe@mun.ca (J. Conliffe).*

17 *Postal address: Dr. James Conliffe,*

18 *Department of Earth Sciences,*

19 *Memorial University of Newfoundland,*

20 *St John's, Newfoundland,*

21 *A1B 3X5, Canada*

22 *Phone Number: (001) 709 7373986*

23 *Fax Number: (001) 709 7372589*

24

25

26 **Reference**

27 *Conliffe, J., Azmy, K., Gleeson, S.A. and Lavoie, D. (2010) Fluids associated with*
28 *hydrothermal dolomitization in St. George Group, western Newfoundland, Canada.*
29 *Geofluids 10(2), 422-437; DOI: 10.1111/j.1468-8123.2010.00295.x*

30

31 **Abstract**

32 Dolomite reservoirs are increasingly recognised as an important petroleum exploration
33 target, although the application of a hydrothermal dolomite exploration model to these
34 reservoirs remains controversial. The St. George Group of western Newfoundland
35 consists of a sequence of dolomitised carbonates, with significant porosity development
36 (up to 30%) and petroleum accumulations. Fluid-inclusion microthermometry and bulk
37 fluid leach analyses indicated that fluids responsible for matrix dolomitization (associated
38 with intercrystalline porosity) and later saddle dolomitization are $\text{CaCl}_2 \pm \text{MgCl}_2$ rich
39 high salinity (up to 26 eq. wt% NaCl) brines. Integration of fluid inclusion data with
40 thermal maturation histories from the St. George Group show that these dolomites
41 formed at temperatures higher than the ambient rock temperature, and are therefore
42 hydrothermal in origin. Bulk leach analyses show that dolomitization is associated with
43 influxes of post-evaporitic brines (\pm Cl enriched magmatic fluids) late in the diagenetic
44 history of these carbonates. This dolomitization is possibly Devonian in age, during a
45 period of significant magmatic activity, extensional tectonics and development of
46 hypersaline basins. Petrographic and geochemical similarities between Paleozoic hosted
47 hydrothermal dolomitization in western Newfoundland, eastern Canada and the

48 northeastern United States are consistent with a regional scale hydrothermal
49 dolomitization event late in the diagenetic history of these carbonates.

50

51

52 **Introduction**

53 Hydrothermal dolomites (HTD) reservoirs have increasingly been recognised as an
54 important exploration target (Davies and Smith, 2006). These dolomites have been
55 reported from a large number of locations worldwide e.g. the Paleozoic basins of eastern
56 Canada and the United States (Smith, 2006; Lavoie and Chi, in press; Lavoie et al., in
57 press a), Devonian carbonates of the Western Canada sedimentary basin (Qing and
58 Mountjoy, 1994; Al-Aasm, 2003), Jurassic basins along rifted Atlantic margins
59 (Wierzbicki et al., 2006) and Carboniferous carbonates of the Iberian Belt, Spain
60 (Gasparini et al., 2006). Hydrothermal dolomitization is defined as dolomitization
61 occurring under burial conditions by high salinity fluids at temperatures higher than the
62 ambient temperature of the host formation (Davies and Smith, 2006). Davies and Smith
63 (2006) suggest that transtensional seismic platform sags associated with major structural
64 features (extensional and/or strike-slip faults) which act as a focus for the HTD fluids
65 should be targeted in exploration programs. However, the interpretation of these
66 dolomites as hydrothermal remains controversial and has been criticized by a number of
67 authors (Machel and Lonnee, 2002, 2008; Lonnee and Machel, 2006; Friedman, 2007).
68 These criticisms centre on a number of questions and uncertainties which remain
69 associated with the HTD exploration model, including determining the absolute timing of
70 dolomitization, the source of Mg^{2+} rich saline brines and the possible driving mechanisms
71 for hydrothermal circulation (Machel and Lonnee, 2002; Davies and Smith, 2006; Lavoie
72 and Chi, in press). From an exploration standpoint these questions need to be addressed
73 in order to determine if the HTD exploration model described by Davies and Smith
74 (2006) is valid and useful.

75 Over the past few years a large number of interpreted HTD reservoirs have been
76 described from the Paleozoic Appalachian Basins of eastern Canada and the northeastern
77 United States (Montanez and Read, 1992; Lavoie and Morin, 2004; Lavoie et al., 2005;
78 Lavoie and Chi, 2006; Smith, 2006; Azmy et al., 2008, 2009; Conliffe et al., 2009;
79 Lavoie and Chi, in press; Lavoie et al., in press a). A number of possible sources have
80 been suggested for the Mg^{2+} -rich fluids responsible for hydrothermal dolomitization,
81 including the drawdown of postevaporite residual brines from overlying Silurian
82 evaporites (Coniglio et al., 1994) and brines circulating through mafic volcanic and
83 ophiolitic basement rocks (Lavoie and Morin, 2004; Lavoie and Chi, 2006; Lavoie and
84 Chi, in press; Lavoie et al., in press b). However, there is still considerable uncertainty
85 about the source of Mg^{2+} -rich fluids. This study aims to constrain the origin and timing of
86 the fluids responsible for replacement and saddle dolomitization in the Lower Ordovician
87 St. George Group, Western Newfoundland. This sequence of dolomitized carbonates has
88 been described as a potential HTD petroleum reservoir (Cooper et al., 2001; Azmy et al.,
89 2008, 2009; Conliffe et al., 2009). The dolomites of the St. George Group are commonly
90 associated with intracrystalline and vuggy porosity (Knight et al., 2007, 2008), and these
91 porous horizons are currently the driver for renewed petroleum exploration (Cooper et al.,
92 2001). Recent drilling on the Port au Port Peninsula have encountered horizons with
93 significant porosity in the Aguathuna (9.8% porosity and 21 mD permeability over 9.8m),
94 Catoche Formation (15 m of 8.7% average porosity) and Watts Bight Formation (up to
95 30% porosity, with a mean 14% over 44.5m), which are associated with dolomitization of
96 the predominantly low porosity and permeability rocks of the St. George Group
97 carbonates.

98 This is the first study in the Appalachian Basin to integrate petrography with detailed and
99 comprehensive fluid inclusion and bulk fluid inclusion (anion and cation) analyses. Fluid
100 inclusion analyses provide important constraints on the temperature of dolomitization and
101 combined with stable isotope analyses can help to define the nature and origin of the
102 dolomitizing fluids. Anion ratios (especially Cl/Br) are particularly useful in determining
103 the source of fluids (e.g. Walter et al., 1990; Kesler et al., 1995), as Cl and Br act
104 conservatively in solution and, with the exception of halite dissolution, water-rock
105 interaction does not alter Cl/Br ratios (e.g. Rittenhouse, 1967; Carpenter et al., 1978).
106 These data are combined with information on the thermal maturity and burial history of
107 the St. George Group, and are used to determine the source of these fluids and whether
108 they are truly hydrothermal (according to the criteria of Machel and Lonnee, 2002 and
109 Davies and Smith, 2006). Economically this has important implications for the HTD
110 exploration model that is currently being used from Western Newfoundland to the
111 Appalachian Basin in eastern USA.

112

113 **Geological Setting**

114 The Lower Paleozoic shelf rocks of western Newfoundland comprise a succession of
115 Cambrian to Devonian siliciclastic and carbonate sediments that outcrop over 400km
116 from Cape Norman in the north to the Port au Port Peninsula in the south (Fig. 1). These
117 shallow- to deep-marine successions were deposited on the southern margin of Laurentia
118 during the Late-Proterozoic break-up of Rodinia and record the evolution of the margin
119 from a long-lived (~50Ma) passive margin (Labrador, Port au Port and St. George

120 Groups) to an active foreland basin (Table Head Group) (James et al., 1989; Stenzel et
121 al., 1990; Cooper et al., 2001; Waldron and van Staal, 2001; van Staal, 2005).

122 The St. George Group consists of a ~500 to 600m succession of subtidal and peritidal
123 carbonates which were deposited as part of a broad low-energy passive margin platform
124 during the Lower to earliest Middle Ordovician. The group has been subdivided into the
125 Watts Bight, Boat Harbour, Catoche and Aguathuna formations (Knight and James, 1987;
126 Fig. 2). These represent two long-lived Tremadoc and Arenig sequences, which were
127 termed megacycles by Knight and James (1987). The lower megacycle consists of the
128 Watts Bight Formation and most of the Boat Harbour Formation, and is bounded at the
129 top by a regional disconformity, the Boat Harbour Disconformity (BHD; Fig. 2). The
130 upper megacycle comprises of the top of the Boat Harbour Formation, and the Catoche
131 and Aguathuna formations. A regional unconformity with karst features, the St. George
132 Unconformity, marks the top of the St. George Group.

133 Each of these megacycles is attributed to eustatic sea level fluctuations and local
134 tectonics (Knight and James, 1987). These large-scale cycles have a thin lower peritidal
135 interval, a thick middle subtidal succession and a thick upper peritidal cap (Knight and
136 James, 1987; Fig. 2). The peritidal units consist of meter-scale, upward shallowing cycles
137 of thinly bedded peloidal mudstones to packstones which commonly include horizons of
138 stromatolitic, thrombolitic and microbial boundstone mounds (Knight et al., 2007, 2008).
139 The subtidal layers are more thickly bedded (~5m) and are comprised of intensely
140 bioturbated peloidal wackestones to mudstones, parallel laminated peloidal packstones to
141 grainstones and large thrombolitic boundstone mounds (Knight et al., 2007, 2008).

142

143 **Dolomitization and diagenesis of the St George Group**

144 Petrographic examination of the St. George Group carbonates has led to the recognition
145 of at least three main generations of dolomite in all the units, occurring as both
146 replacements and cements and recording multiple phases of dolomitization (Azmy et al.,
147 2008, 2009; Greene, 2008; Conliffe et al., 2009). The earliest dolomite (D1) replaces
148 precursor calcite (C1) and early meteoric calcite cements (C2). D1 is a fine grained (4 to
149 40 μ m) dolomicrite which is fabric-retentive and suggests that dolomitization started
150 shortly after inception of burial, at low temperatures during the early stages of diagenesis.
151 Trace element geochemistry and stable isotope analysis suggested a mixed of marine and
152 meteoric source for D1 dolomitizing fluids, possibly in a mixing zone environment
153 (Azmy et al., 2008, 2009).

154 Later-stage replacement dolomites (D2) consist of coarse, (50 to 300 μ m) equant sub- to
155 euhedral dolomite rhombs with characteristic cloudy cores and clear rims (Fig. 3a). The
156 $\delta^{18}\text{O}_{\text{fluid}}$ of D2 ranges from -2 to 5‰ VSMOW), which are typical of influxes of basinal
157 brines (Goldstein and Reynolds, 1994). Petrographic studies of the St. George Group
158 dolomites have shown that significant intercrystalline porosity (up to 10%) resulted from
159 D2 dolomitization (Azmy et al., 2008, 2009; Conliffe et al., 2009).

160 The latest dolomite generation (D3) consists of pore- and fracture-filling to locally
161 replacive coarse sub- to anhedral crystals (>0.5mm). D3 dolomite in the St. George
162 Group is commonly Fe-rich (up to 20000ppm) and has the most enriched $\delta^{18}\text{O}$ signature
163 of dolomitizing fluids (3 to 8‰ VSMOW), which is consistent with late, deep burial or
164 hydrothermal fluids (Tucker and Wright, 1990; Goldstein and Reynolds, 1994; Azmy et
165 al., 2008, 2009; Conliffe et al., 2009). A translucent, coarse blocky calcite cement (C3) is

166 the last diagenetic phase recorded in the St. George Group carbonates and partly to
167 completely fills pores and fractures still open after D3 precipitation (Fig. 3b). Although
168 some dissolution and vuggy porosity has been reported associated with D3 dolomitization
169 (Azmy et al., 2008, 2009) these vugs are rarely interconnected, and D3 and C3 cements
170 are generally associated with a reduction in the effective porosities of these early
171 dolomites (Azmy et al., 2008, 2009; Conliffe et al., 2009).

172

173 **Methodology**

174 Samples for analyses were collected from outcrops at Isthmus Bay on the Port au Port
175 Peninsula and Barbace Cove on the Port aux Choix Peninsula, as well from a number of
176 exploration drillholes (RND 001 and RND 002 on the Port au Port Peninsula and PC79-
177 02 on the Port aux Choix Peninsula (cf. Azmy et al., 2008; Greene, 2008, Azmy et al.,
178 2009; Conliffe et al., 2009). The analyzed samples were carefully selected from a suite of
179 samples that were collected at high resolution intervals of $\sim 2\text{m}$ ($\pm 0.5\text{m}$) and represent a
180 complete succession ($\sim 525\text{m}$) of the St. George Group (cf. Azmy et al., 2008, Greene,
181 2009; Azmy et al., 2009, Conliffe et al., 2009). The sample locations are the same as
182 those presented in Knight et al. (2007, 2008) and the numbering scheme used by these
183 authors is retained here. Based on petrographic and geochemical investigations doubly
184 polished wafers ($\sim 100\mu\text{m}$ thick) for fluid inclusion analyses were prepared from
185 representative samples of D2, D3 and C3. Microthermometric fluid-inclusion analyses
186 were performed using a Linkam THMSG600 heating-freezing stage calibrated with
187 synthetic H_2O and CO_2 fluid inclusion standards (Syn Fliinc, USA) at temperatures
188 between -56.6 and 374.1°C . Precision on the measurements is $\pm 0.2^\circ\text{C}$ at -56.6°C and \pm

189 1°C at 300°C. Homogenization temperatures were recorded first in order to minimise the
190 effects of stretching in relatively soft minerals such as calcite. Following procedures
191 outlined by Shepherd et al. (1985) the initial melting temperatures (T_i), hydrohalite
192 melting ($T_m(\text{hh})$), last ice melting ($T_m(\text{ice})$) and the temperature of homogenization (T_h)
193 were measured in two-phase (liquid + vapour) inclusions hosted in dolomite and calcite.
194 Hydrohalite melting temperatures facilitate estimates of fluid compositions based on
195 microthermometric data, particularly when combined with charge balance calculations
196 from crush leach analyses. However care must be taken in interpreting these ratios as no
197 phase diagrams are available which accurately describe the $\text{H}_2\text{O}-\text{NaCl}-\text{CaCl}_2-\text{MgCl}_2$
198 system, and the small size of these inclusions which led to the recording of hydrohalite
199 melting being challenging. Salinities were calculated from the $T_m(\text{hh})$ and $T_m(\text{ice})$ using a
200 program by Chi and Ni (2006) for the system of $\text{H}_2\text{O}-\text{NaCl}-\text{CaCl}_2$. X_{NaCl} was calculated
201 using the equation of Oakes et al. (1990).

202 Following fluid inclusion microthermometry, specific dolomite and calcite phases were
203 selected and cut from a polished mirror-image slab of each fluid inclusion wafer for
204 crush-leach analyses. Care was taken to select samples dominated by one population of
205 primary fluid inclusions. These samples were prepared for crush-leach analysis following
206 the procedure of Banks and Yardley (1992) and Gleeson and Turner (2007). The samples
207 were crushed and sieved to give a 1-2 mm grain size fraction. After crushing, the samples
208 were hand picked under a binocular microscope to obtain 2 g of a clean mineral separate.
209 The samples were washed in 18.2 m Ω water and heated overnight on a hot plate, then
210 dried in an oven. Finally ~1 g of sample was ground to a fine powder in an agate mortar
211 and pestle. The powder was transferred to an unreactive vial and 5 mL of clean water

212 was added. These samples were shaken, and filtered through 0.2 micron filters. The
213 resultant leachate was analysed for anions (Cl, Br, F and sulphate) using a Dionex DX600
214 ion chromatograph (IC) at the University of Alberta. The detection limits for all anions
215 was 0.008 ppm. Replicate analyses of standards and samples yielded data with a
216 reproducibility of 5%. Na, K and Li were analysed on the same leachate using atomic
217 adsorption spectroscopy (AAS). The detection limits for these cations was 0.002 ppm.

218 As the total number of inclusions in each sample is unknown the ion concentrations
219 measured in the leachates do not represent the concentrations in the basinal fluids. In
220 order to back-calculate the ion concentrations in the fluids, the crush leach data were
221 normalized to the salinity values as measured by microthermometry using the technique
222 described in Banks et al. (2002). In addition, a charge balance calculation (see Shepherd
223 et al., 1985) was carried out for each sample. In a solution with a neutral charge the
224 number of positively charged ions (cations) should equal the number of negatively
225 charged ions (anions) and should yield a charge balance of 1. Any deviation from this
226 value can indicate contamination from the host mineral and/or certain cations and anions
227 have been omitted from the analysis. Our charge balance calculations use Cl, Br, F, SO₄,
228 Na, K and Li compositions of the carbonate-hosted leachates. However Ca, Mg, CO₃ and
229 HCO³⁻ are excluded from the analyses due to possible contamination from the host
230 carbonates. Therefore the charge balances presented below are incomplete and are solely
231 used to identify variations in fluid compositions.

232

233 **Results of Fluid Inclusion Analyses**

234 A number of fluid inclusion microthermometric studies have been published on the St.
235 George Group carbonates (Azmy et al., 2008, 2009; Conliffe et al., 2009) but there has
236 been no comprehensive fluid inclusion study of hydrothermal dolomites in Western
237 Newfoundland. This study combines previously published fluid inclusion data from the
238 Aguathuna (Azmy et al., 2008), Boat Harbour (Azmy et al., 2009) and Watts Bight
239 (Conliffe et al., 2009) formations with new microthermometric data from D2 and D3
240 dolomite, and C3 calcite in the Catoche, Boat Harbour and Watts Bight formations (Table
241 1).

242 **Fluid inclusion petrography and classification**

243 The fluid inclusions in dolomite (D2 and D3) were hosted in clusters in the core of
244 dolomite crystals or in discrete zones within dolomite rhombs and inclusions were
245 commonly elongate in the direction of growth. Inclusions in C3 calcite were found in
246 clusters in the core of crystals and can be very large with respect to their host crystals (up
247 to 50 μ m; Fig. 3f). Therefore inclusions in dolomite and calcite are considered primary in
248 origin and represent samples of fluid trapped during growth (Goldstein, 2003). Primary
249 fluid inclusion assemblages in D2 and D3 dolomite are characterised by a consistent
250 degree of fill (liquid/vapour ratio) indicating little or no post-entrapment reequilibrium
251 (leaking or necking down of inclusions). In contrast some primary inclusion in C3 calcite
252 show evidence of post-entrapment leaking and/or stretching (e.g. microfractures at edge
253 of inclusions). Care was taken only to record microthermometric data from inclusions
254 which displayed small T_h variations within an individual inclusion assemblage, usually
255 less than 10°C, suggesting that post-entrapment effects are not important (Goldstein and
256 Reynolds, 1994).

257 D2 dolomite

258 The fluid inclusions in D2 dolomite are biphasic (liquid + vapour; L + V) and range in
259 size from 2 to 20 μ m. The initial melting temperatures (T_i) ranged from -55.3 to -48 $^{\circ}$ C
260 (Table 1), corresponding to the eutectic temperature for the H₂O-NaCl-CaCl₂ \pm MgCl₂
261 system (Shepherd et al., 1985). Very low melting temperatures were recorded in one
262 sample from the Catoche Formation (MG13); this is attributed to metastable melting
263 phenomenon in the H₂O-NaCl-CaCl₂-MgCl₂ system. An additional phase change
264 occurred at \sim -40 to -30 $^{\circ}$ C in some samples from the Catoche and Watts Bight formations.
265 This is interpreted as hydrohalite (NaCl.2H₂O) melting and indicates that these fluids are
266 CaCl₂ rich (Oakes et al., 1990), yielding Ca:Na ratios of 7:1 to 9:1 for the Catoche
267 Formation and 2:1 to 6:1 for the Watts Bight Formation. Ice melting temperatures
268 ($T_m(\text{ice})$) ranged from -26.7 to -6.2 $^{\circ}$ C, which yield a wide range of fluid salinities of
269 (10.1 to 24.8 eq. wt% NaCl + CaCl₂; Fig. 4).

270 Inclusions in D2 dolomite homogenize (T_h) to the liquid phase between 60 and 121 $^{\circ}$ C.
271 However there are significant variations in homogenization temperatures between sample
272 in each formation (Fig. 4), with samples from the Aguathuna and Watts Bight formations
273 having lower T_h ($74 \pm 3^{\circ}$ C and $83 \pm 12^{\circ}$ C respectively) than samples from the Catoche
274 Formation ($107 \pm 13^{\circ}$ C) and the Boat Harbour Formation ($102 \pm 15^{\circ}$ C).

275 D3 dolomite

276 The fluid inclusions in D3 dolomite are two-phase (L + V) and range in size from 2 to
277 20 μ m. The eutectic temperature of -66 to -50.2 $^{\circ}$ C indicates the presence of CaCl₂ \pm
278 MgCl₂ in solution. Hydrohalite melting temperatures were recorded in some larger
279 inclusions in D3 and range from -31.5 to -30.2 $^{\circ}$ C. Assuming a pure CaCl₂-NaCl fluid

280 composition this corresponds to a Ca:Na ratio of ~ 2:1. $T_m(\text{ice})$ ranged from -1 to -
281 31.3°C, with calculated salinities from 1.7 to 26.2 eq. wt% NaCl + CaCl₂. Inclusions
282 homogenize (T_h) to the liquid phase between 69 and 140°C (mean = 111°C, standard
283 deviation = 15°C), with no significant variations found between the formations.

284 **C3 calcite**

285 Fluid inclusions in C3 calcite display a wide range of size (2 to 50µm) and degree of
286 liquid fill (0.6 to 0.95). Low T_i of -62 to -49°C again suggests that Na, Ca and Mg are the
287 dominant cations in solution. The majority of inclusions in C3 calcite have salinities of
288 17 to 24 wt% NaCl + CaCl₂ and have T_h values of 64 to 182°C.

289

290 **Results of Bulk Fluid Analyses**

291 Following detailed petrographic and microthermometric analyses, fourteen samples (nine
292 D2, three D3 and two C3) were selected for bulk fluid analyses. The results of the
293 leachate analysis are summarized in Table 2, and the calculated charge balances and
294 molar element ratios are presented in Table 3.

295 **D2 dolomite**

296 The crush leach analyses of the D2 dolomite samples suggest that there are two
297 geochemically-distinct fluids in this paragenetic phase; one is found in samples above the
298 BHD (Aguathuna and Catoche formations) and the other in those below the BHD (Boat
299 Harbour and Watts Bight formations).

300 The charge balances of D2 dolomite leachates from above the BHD range from 0.5 to
301 0.8. Leachate analyses of D2 samples from below the BHD have a charge balance of 1 or
302 a slight excess in cations (1.0 to 1.5). The anion analyses of samples from above and

303 below the BHD are also markedly different. D2 samples from carbonates above the BHD
304 have Cl/Br ratios of 167 to 284, significantly less than 655 (composition of modern day
305 seawater from the compilation of Fontes and Matray, 1993). In contrast those below the
306 BHD have Cl/Br ratios that are equal to or slightly above that of seawater (661 to 935)
307 and slightly elevated Na/Br ratios (677 to 972). The absolute concentrations of Cl and Br
308 indicate that D2 dolomites above the BHD plot below the Seawater Evaporation Trend
309 (SET), while those from below the BHD lie on or slightly to the left of the SET.

310 The Na/Br and K/Br ratio of leachates (Fig. 7) show that three samples from the Catoche
311 Formation (on the Port a Choix Peninsula) are depleted in K (below the SET). In contrast
312 those from the Aguathuna, Boat Harbour and Watts Bight formations from the Port au
313 Port Peninsula have relatively high K/Br ratios (15.5 to 80.5), higher than the SET and
314 suggesting an addition of K to the fluids. In addition a single sample from the Watts
315 Bight Formation (WBA3) has elevated Li concentrations (Li/Na of 0.0015).

316 **D3 dolomite**

317 The leachate-analyses from D3 dolomites are similar to those of D2 dolomites above the
318 BHD, and no significant variations have been observed between samples from above or
319 below the BHD. A charge balance calculation yields values of 0.5 to 0.6. The Cl/Br ratios
320 from all three D3 samples are 305, and are lower than modern day seawater (Fig. 5).
321 Halide compositions have been calculated for two D3 samples plot below the SET,
322 indicating mixing between high salinity brines and a dilute fluid. These fluids have low K
323 and Li values (Li values below the detection limit), consistent with limited water-rock
324 interaction during fluid transport.

325 **C3 calcite**

326 Only two C3 calcite samples were analysed, one from the Boat Harbour Formation and
327 one from the Watts Bight Formation. Both samples have Cl/Br ratios lower than modern
328 seawater (371 and 538 respectively). Bulk fluid analyses of C3 calcite from the Boat
329 Harbour and Watts Bight formations show significant variations (Table 3; Fig. 7), with
330 variable SO₄/Br, Na/Br and K/Br ratios.

331

332 **Discussion**

333 **Hydrothermal Origin of St. George Group Dolomites**

334 In order to determine whether dolomites are truly hydrothermal or not, the
335 homogenization temperature of dolomites has to be evaluated in light of the burial and
336 thermal history of the dolomite host (Davies and Smith, 2006). If the homogenization
337 temperatures are significantly (5 to 10°C) higher than maximum burial temperatures it
338 can be safely concluded that these dolomites are hydrothermal. However if the
339 homogenization temperatures are the same as, or lower than, maximum burial
340 temperatures then these dolomites cannot be confidently classified as hydrothermal in
341 origin, and may, in fact, be deep burial dolomites which formed at, or below, ambient
342 temperatures (geothermal or hydrofrigid dolomites; Machel and Lonnee, 2002). This
343 rigorous definition of “hydrothermal dolomites” is important in avoiding the
344 misinterpretation of dolomites as hydrothermal dolomites, as demonstrated by Machel
345 and Lonnee (2002) and is necessary for the application of the HTD exploration model (as
346 proposed by Davies and Smith, 2006).

347 Maximum burial temperatures from the St. George Group in western Newfoundland have
348 been indirectly estimated from conodont alteration indices (CAI), acritarch alteration

349 indices (AAI) and random graptolite reflectance data (GRo) (Nowlan and Barnes, 1987;
350 Williams et al., 1998). A general trend of increasing maturity from the Port au Port
351 Peninsula in the south to Cape Norman in the north has been documented. The AAI
352 values from the Watts Bight Formation (lowermost unit of the St. George Group) on the
353 Port au Port Peninsula are 2.3, combined with the low AAI and low GRo from the
354 overlying Ordovician and Carboniferous strata (Williams et al., 1998) indicates that
355 maximum burial temperatures on the Port au Port Peninsula are $<75^{\circ}\text{C}$. The St. George
356 Group on the Port au Choix Peninsula is characterised by higher AAI (>3) and GRo
357 ($>1.11\%$), corresponding to burial temperatures of ~ 120 to 130°C . Nowlan and Barnes
358 (1987) argued that these higher temperatures may be related to elevated geothermal
359 gradients during the passage of north-western Newfoundland over a hot spot during the
360 Mesozoic. However no evidence of elevated geothermal gradients was observed in
361 overlying Carboniferous strata (William et al., 1998). Therefore, these temperatures must
362 have been reached during the Paleozoic and are due to normal orogenic processes (i.e.
363 deep burial and high geothermal gradients).

364 When pristine, fluid inclusion homogenization temperatures reflect the minimum
365 trapping temperature, and therefore the minimum temperature of dolomitization. In order
366 to determine the extent to which these temperatures underestimate the true dolomitization
367 temperature isochores have been constructed for fluids with T_{H} of 70 and 100°C and
368 salinities of 8 and 16 eq. wt% NaCl (Fig. 8) using the program FLUIDS (Bakker, 2003).
369 If dolomitization occurred at a depth of 2-3km (maximum burial depth on the Port au
370 Port Peninsula; Williams et al., 1998), trapping pressures range from 530 to 795 bars for
371 lithostatic pressures and 196 to 294 for hydrostatic pressures (Fig. 8). At these pressures

372 the T_H underestimates the true trapping temperatures by 19-35°C for lithostatic pressures
373 and 7-13°C for hydrostatic pressures. Therefore it can be concluded that although the
374 fluid inclusion homogenization temperatures provide minimum trapping temperatures,
375 these data may severely underestimate the true temperature of dolomitization, particularly
376 at deeper levels (> 2km).

377 The T_H values from D2 and D3 dolomites on the Port au Port Peninsula (Fig. 9) are equal
378 to, or greater than, the maximum burial temperatures estimated by Williams et al. (1998).
379 Therefore D2 and D3 dolomite in the St. George Group on the Port au Port Peninsula can
380 be described as hydrothermal in origin according to the criteria of Machel and Lonnee
381 (2002), particularly if the underestimation of true temperatures of dolomitization based
382 on fluid inclusion homogenization temperatures is considered. In contrast, maximum
383 burial temperatures estimated from the St. George Group on the Port aux Choix Peninsula
384 are equal to or greater than the fluid-inclusion homogenization temperatures in the
385 dolomites (Fig. 9). This may be due to the burial of these dolomites to temperatures
386 which exceed the homogenization temperatures at some point after dolomitization, as has
387 been suggested by Smith (2006) for Ordovician dolomites in New York. Without a
388 precise control on the timing of dolomitization, it cannot be stated unequivocally that the
389 St. George Group dolomites on the Port aux Choix Peninsula are hydrothermal in origin,
390 they may instead have formed at, or below, ambient rock temperatures during deep
391 burial.

392 **Origin of Hydrothermal Fluids**

393 Numerous studies have shown that crush leach analyses, combined with
394 microthermometric data, are useful in the determination of the source of dolomitizing

395 fluids (Banks et al., 2002; Gleeson and Turner, 2007). Fluid inclusion analyses show that
396 dolomitizing fluids in western Newfoundland are high salinity $\text{CaCl}_2\text{-MgCl}_2$ -rich brines
397 (Table 1), similar to other hydrothermal dolomites in eastern Canada and northeastern
398 United States (Coniglio et al., 1994; Lavoie and Morin, 2004; Lavoie et al., 2005; Lavoie
399 and Chi, 2006; Smith, 2006; Lavoie and Chi, in press; Lavoie et al., in press a). However
400 significant variations were recognised in the composition and source of the hydrothermal
401 fluids responsible for D2 and D3 dolomitization, and the precipitation of C3 calcite.

402 *D2 Dolomite*

403 The charge balance calculations for D2 dolomites range from 0.5 to 1.5, with samples
404 from above the BHD having lower charge balances (<1) that those from below the BHD
405 (>1). This may indicate compositional variations between D2 dolomitizing fluids from
406 above and below the BHD. Compositional variation is also indicated by
407 microthermometric data. Hydrohalite melting temperatures, combined with $T_m(\text{ice})$, from
408 D2-hosted inclusions in the Catoche Formation (above the BHD) yield salinities of 20.8
409 to 22.3 eq. wt% NaCl and X_{NaCl} of 0.1 to 0.13 (Fig. 10a). In contrast, the fluids present in
410 D2 dolomite from the Watts Bight Formation (below the BHD) have a range in
411 compositions from high salinity (up to 25 eq. wt% NaCl) Ca-rich (X_{NaCl} of 0.14) fluids to
412 lower salinity (12.4 eq. wt% NaCl), less calcic (X_{NaCl} of 0.28) brines (Fig 10b). This is
413 consistent with fluid mixing between bittern brines similar to those identified in the D2
414 dolomite from above the BHD and a lower salinity NaCl-rich fluid.

415 The halide geochemistry of entrapped fluids in D2 dolomites above the BHD is
416 consistent with genesis from evaporated seawater. These fluids are enriched in Br relative
417 to Cl, with Cl/Br ratios significantly less than that of modern seawater (Fig. 5). This

418 suggests that these fluids formed from seawater that has evaporated to such a degree that
419 halite has precipitated from the solution, which resulted in the residual fluid (or bittern
420 brine) becoming enriched in Br (Carpenter, 1978). This is confirmed by the absolute
421 concentrations of Cl and Br in these samples, which show that these fluids originated as
422 bittern brines which may be partially diluted by meteoric waters (Fig. 6).

423 The Cl/Br ratios of D2 dolomites below the BHD are greater than modern seawater (661
424 to 935; Fig. 5). This suggests that these fluids are not post-evaporitic brines (Chi and
425 Savard, 1997) and fluids with Cl/Br ratios greater than seawater are generally assumed to
426 have a component which is derived from the dissolution of halite (Walter et al., 1990;
427 Kesler et al., 1995). However, fluids associated with halite dissolution are commonly Mg
428 poor, as co-precipitation of Mg^{2+} with NaCl is negligible (McCaffery et al., 1987), and
429 are, therefore, unlikely to be associated with the dolomitization of significant volumes of
430 rock. Therefore an alternative source for the substantial volumes of Mg^{2+} for
431 dolomitization must be sought for these fluids. Dissolution of Mg-rich salts, including
432 polyhalite ($K_2MgCa_2(SO_4)_4 \cdot 2H_2O$) and carnallite ($K_2MgCl_3 \cdot 6H_2O$) is a possible source
433 of Mg^{2+} to these fluids (Warren, 2000). A number of previous studies have identified
434 chert nodules in these carbonates, the former possibly being of evaporitic in origin,
435 particularly where associated with the BHD (Pratt, 1979) and in the Aguathuna
436 Formation (Pratt and James, 1986). However, the rarity of these nodules indicates that
437 dissolution of magnesium-rich salts was minor at most. Other possible sources for
438 magnesium-rich fluids include structural Mg^{2+} expelled during interactions with clay
439 minerals (e.g. illitization of clay minerals; Boles and Franks, 1979; Warren 2000) and

440 mafic to ultramafic igneous units. However no such water rock interactions were evident
441 in the cation analyses of these fluids (see below).

442 Lavoie and Morin (2004) and Lavoie and Chi (2006, in press) noted that some Lower
443 Silurian hydrothermal dolomites in Eastern Canada were spatially associated with Lower
444 Ordovician ultramafic slivers and within-plate mafic volcanic units. Moreover, an
445 empirical link between foreland basins and tectono-magmatic events at the continental
446 margin of Laurentia with hydrothermal dolomitization has been proposed for the
447 carbonates of the Middle-Upper Ordovician (Taconian foreland), Silurian (Salinic
448 foreland) and Lower Devonian (Acadian foreland) (Lavoie and Chi, in press; Lavoie et
449 al., in press a). Although magmatic fluids generally have low Mg:Ca ratios (<0.47;
450 Smith et al., 1995; Graser et al., 2008), they are capable of dolomitization at the elevated
451 fluid temperatures encountered in hydrothermal dolomites (Hardie 1987; Lavoie et al, in
452 press a). Magmatic processes may also enhance convective circulation of dolomitizing
453 fluids in sedimentary basins, and Lavoie and Chi (in press) considered that magmatic
454 activity associated with active foreland basins (e.g. Western Newfoundland during the
455 Ordovician) are likely to be associated with the development of HTD reservoirs.
456 Therefore, magmatic fluids are considered a possible source for Mg²⁺-rich fluids
457 associated with hydrothermal dolomitization below the BHD.

458 *D3 Dolomite*

459 Dolomitizing fluids associated with D3 saddle dolomites from both the Port au Port and
460 Port aux Choix peninsula are characterised by similar microthermometric characteristics
461 and bulk fluid geochemistry. Primary fluid inclusions in D3 dolomites are CaCl₂ rich
462 fluids (X_{NaCl} of 0.22 to 0.34) with a narrow range of T_{H} values ($111 \pm 15^{\circ}\text{C}$). These fluids

463 are similar to high salinity (up to 30 eq. wt% NaCl) CaCl₂-rich mineralizing fluids
464 associated with MVT mineralization in the Appalachian Basin, including the Daniels
465 Harbour Pb-Zn mine in Western Newfoundland (Lane, 1990; Appold et al., 1995). All
466 bulk fluid analyses from the Aguathuna, Catoche and Boat Harbour formations have
467 Cl/Br ratios of 305, suggesting that these fluids also originated as bittern brines.
468 However, absolute Cl and Br concentrations indicate that these fluids formed from the
469 mixing of brines with dilute fluids, such as meteoric water (Fig. 6), consistent with the
470 wide range of salinities of D3 fluids (1.7 to 26.2 eq. wt% NaCl). Bulk fluid analyses of
471 sphalerite from the Daniel Harbour mine also show evidence of mixing between high
472 salinity bittern brines and low salinity, possible meteoric, fluids (Kessler et al. 1996). The
473 similarities in the microthermometric characteristics and bulk fluid composition support
474 the link between D3 dolomitization and MVT mineralization in Western Newfoundland.

475 *C3 Calcite*

476 Fluids associated with C3 calcite precipitation are also Ca-rich brines, with Cl/Br ratios
477 lower than modern seawater (371 to 538) indicating that these fluids formed from
478 evaporated seawater. However microthermometric analyses show that these fluids have a
479 wide range X_{NaCl} (0.1 to 0.54) and salinities of 17.9 to 22.8 eq. wt% NaCl (Fig. 10d),
480 consistent with either mixing between Ca-rich and Na-rich fluids or multiple episodes of
481 late-stage calcite precipitation. Based on bulk fluid analyses, which show that included
482 fluids in C3 calcite from the Boat Harbour and Watts Bight formations are geochemically
483 distinct, it is likely that C3 calcite represent a number of separate episodes of calcite
484 precipitation in Western Newfoundland. This is consistent with trace element

485 geochemistry and CL petrography from C3 calcites (Azmy et al., 2008, 2009; Conliffe et
486 al. 2009).

487 **Evidence for Water-Rock Interactions along the Flow Path**

488 Unlike geochemically conservative anions, the concentrations of reactive cations (Na, K
489 and Li) are easily altered during interaction with the host rocks (Banks et al., 2002) and
490 therefore are useful in determining the extent and type of water-rock interactions. In
491 Figure 7 it is shown that D2 samples from the Port au Port Peninsula (Aguathuna, Boat
492 Harbour and Watts Bight formations) are enriched in K relative to samples from Catoche
493 Formation on the Port aux Choix Peninsula. Although the exact cause of this K
494 enrichment is unclear, it is possibly due to water-rock interactions (e.g. albitization of K-
495 feldspars; Banks et al., 2002). The variability of K enrichment from the Port au Choix to
496 the Port au Port Peninsula may reflect variations in the local geology; with dolomitizing
497 fluids on the Port au Port Peninsula flowing along fault conduits through the clastic
498 sediments of the Goose Tickle Group (see Cooper et al., 2001, pg 412).

499 With the exception of a single sample from the Watts Bight Formation, all other samples
500 have relatively low Li (Li/Na of <0.0006). Micas are a major reservoir for crustal Li
501 (Banks et al., 2002), and therefore the low Li content of these fluids suggests that the
502 effects of any interaction with clay minerals is generally minimal when compared with
503 other studies (e.g. Gleeson and Turner, 2007; Vandeginste et al., 2009).

504 The dolomitizing fluids associated with D3 dolomite precipitation are depleted in K and
505 Na relative to the evaporitic composition of modern-day seawater, which may be related
506 to albitization of Ca-bearing feldspars, as has been observed in previous studies (e.g.
507 Gleeson and Turner, 2007). This is in contrast to D2 dolomites from the Port au Port

508 Peninsula, and suggests that D3 dolomitizing fluids on the Port au Port Peninsula had a
509 different evolution or flow path from that of D2 dolomitizing fluids.

510 **Implication for the HTD exploration model in Palaeozoic Appalachian Basins**

511 Although petroleum fluid inclusions have not been recorded in D2 or D3 dolomite, D2
512 dolomite rhombs are commonly coated by a bituminous material (Conliffe et al. 2009),
513 indicating that petroleum migration may have occurred after D2 dolomitization, and
514 therefore the St. George Group dolomites are potential hydrocarbon reservoirs.
515 Significant accumulations of petroleum in dolomite reservoirs have been recorded in the
516 Palaeozoic Appalachian Basins of eastern Canada and the northeastern United States (e.g.
517 the Upper Ordovician Trenton Black River Group in south-central New York, the Lower
518 Ordovician Garden Hill oil field on the Port au Port peninsula in western Newfoundland
519 and the Lower Devonian Galt gas field on Gaspé Peninsula, Quebec) and an HTD
520 exploration model for these reservoirs has been proposed by a number of studies (e.g.
521 Cooper et al., 2001; Smith, 2006). However the application of the HTD exploration
522 model in the Appalachians remains controversial and the definition of dolomite reservoirs
523 as hydrothermal has been the subject of a number of criticisms (Machel and Lonnee,
524 2002, 2008; Lonnee and Machel, 2006; Friedman, 2007). The recognition of
525 hydrothermal dolomite reservoirs must be based on integration of fluid inclusion
526 homogenization temperatures with documented geothermal and/or burial histories
527 (Machel and Lonnee, 2002; Davies and Smith, 2006). Most fluid inclusion
528 homogenization temperatures from matrix and saddle dolomites in the Appalachians
529 range from 80 to 170°C and are greater than maximum burial temperatures, consistent
530 with the description of these dolomites as hydrothermal in origin (Lavoie et al., 2005;

531 Smith, 2006; Lavoie and Chi, in press; this study). Therefore, both matrix and saddle
532 dolomites are here considered to be hydrothermal in origin, although they are not
533 necessarily cogenetic.

534 HTD dolomite reservoirs in the Appalachian Basins are characterised by multiple phases
535 of dolomitization, with early matrix dolomitization (similar to D2 dolomitization)
536 followed by later saddle dolomite precipitation (D3 dolomite). Saddle dolomite is
537 commonly associated with Mississippi-Valley type mineralization in the Appalachian
538 Orogen (Kesler and van der Pluijm 1990). In addition, fluid inclusions and geochemical
539 evidence highlights similarities between fluids responsible for dolomitization, which have
540 a $\text{MgCl}_2\text{-CaCl}_2\text{-NaCl}$ brine composition and similar stable isotope characteristics (Smith,
541 2006; Azmy et al., 2008, 2009; Conliffe et al., 2009; Lavoie and Chi, in press). The
542 simplest interpretation of the geological and geochemical similarities between these
543 hydrothermal dolomites in the Appalachians is that they are either coeval, or at least
544 represent hydrothermal dolomitization via comparable processes. Therefore, a HTD
545 exploration model may be applicable in Western Newfoundland, throughout the
546 Appalachian and Michigan Basins and in other active foreland basins.

547 The exact timing of these hydrothermal fluid influxes in Western Newfoundland is
548 unknown. Kesler and van der Pluijm (1990) argued that MVT mineralization in the
549 Appalachians, including mineralization at Daniels Harbour, predates late Devonian
550 deformation and therefore hydrothermal dolomitization must have occurred between the
551 Middle Ordovician and the Middle Devonian. Rb-Sr dating of the MVT mineralization at
552 Daniels Harbour, Western Newfoundland proved inconclusive (Nakai et al., 1993).
553 However Rb-Sr dating of MVT deposits in elsewhere in the Appalachians yielded

554 Devonian ages (347 ± 20 Ma and 377 ± 29 Ma; Nakai et al., 1993), and based on the
555 geological and geochemical similarities between MVT deposits throughout the
556 Appalachian Basin (Kesler and van der Pluijm, 1990; Kesler et al. 1996) MVT
557 mineralization in Daniels Harbour (and D3 dolomitization) may also be Devonian in age.
558 D2 matrix dolomitization predates D3 dolomitization, and therefore it must have occurred
559 between the Middle Ordovician and the Devonian. Smith (2006) argued that matrix
560 dolomitisation in the Middle-Upper Ordovician Trenton-Black River (TBR) groups in
561 New York was early in the burial history, as most of the faults associated with
562 dolomitisation were active during the Ordovician and were sealed off by the Upper
563 Ordovician Utica Shale that stratigraphically overlies the TBR. In the Appalachian basin,
564 only minor evaporite nodules have been recorded in Ordovician strata and therefore the
565 large volume of Mg^{2+} for the proposed early matrix dolomitization has to originate from a
566 non-evaporite source. Late Silurian evaporites are preserved in the Michigan basin
567 (Coniglio et al., 1994), but given the interpreted early origin of the dolomitization for the
568 Trenton carbonates (Davies and Smith, 2006), they likely did not source the magnesium
569 for the dolomitization. The potential for fluids derived from or having chemically
570 exchanged with the underlying Precambrian basement is currently touted by some
571 research groups (Selleck, 2006). . The same fundamental problem of Mg^{2+} source for the
572 St. George Group D2 and D3 dolomites exists if an Ordovician dolomitization event is
573 assumed. However, in Western Newfoundland, the Devonian basins show evidence of
574 periodic episodes of evaporation (Burden et al., 2002), providing a possible source of
575 post-evaporitic brines that could have provide the magnesium for both D2 and D3
576 dolomitization if a Devonian age for dolomitization is confirmed. These Mg-rich brines

577 could have been drawn into the underlying sediments via brine reflux, where dense
578 hypersaline brines displace the less dense waters in underlying sediments and seep
579 downwards into the basin. Saline fluids would have subsequently been entrained in
580 hydrothermal convection cells (driven by Devonian igneous activity associated with the
581 Acadian orogeny), possible with some input of magmatic fluids. HTD reservoirs in
582 western Newfoundland are spatially associated with major extensional faults, which were
583 active in the Devonian (e.g. the Garden Hill discovery in the footwall the high angle
584 Round Head Fault; Cooper et al., 2001), and both matrix and saddle dolomites are
585 commonly associated with local fault networks (Knight et al., 2007). Therefore, these
586 major extensional faults are considered to be the main conduits for dolomitising fluids in
587 the St. George Group carbonates (as suggested by Cooper et al., 2001). Some significant
588 differences (petrography, abundance of dolomite phases, Sr isotopes) have been recorded
589 between hydrothermal dolomite reservoirs in the Ordovician of eastern Canada (e.g.
590 between heavily tectonized western Newfoundland successions and the little deformed
591 Anticosti Basin; Lavoie et al., 2005; Azmy et al., 2009), these could be attributable to the
592 very different tectonic framework or possibly to a different timing of dolomitization that
593 proceeded from different fluids. Analyses of Mg isotopes from interpreted hydrothermal
594 dolomites of various ages and tectonic settings are currently being carried out, with the
595 ultimate goal to identify the source of magnesium needed for the huge volume of high
596 temperature dolomites in the Appalachian Basin (Lavoie et al., in press b). Nonetheless,
597 the hydrothermal dolomitization model proposed here is analogous to models proposed in
598 the northeastern United States (e.g. Smith, 2006) and eastern Canada (Lavoie and Chi, in

599 press), and points to regional scale hydrothermal dolomitization throughout the
600 Appalachian Basin.

601

602 **Conclusions**

603 On the basis of fluid inclusion microthermometry and bulk fluid inclusion (anion and
604 cation) analyses, matrix and saddle dolomites in western Newfoundland can be classified
605 as hydrothermal in origin (according to the definition of Machel and Lonnee, 2002 and
606 Davies and Smith, 2006). Bulk fluid analyses indicated that the majority of dolomitizing
607 fluids were post-evaporitic in origin, with some input of Cl enriched fluids below the
608 BHD, which eliminates the mass balance problems envisioned by Machel and Lonnee
609 (2002). We propose that dolomitization was associated with the drawdown of post-
610 evaporitic brines from overlying basins via brine reflux (possibly Devonian). These fluids
611 were then entrained in hydrothermal convection cells driven by magmatic activity
612 (possibly with some input of magmatic fluids), and major extensional faults were the
613 main conduits for dolomitising fluids. The secondary porosity development associated
614 with hydrothermal dolomitization would have facilitated the accumulation of petroleum,
615 and similar settings must be considered prime targets for future HTD exploration, both in
616 Western Newfoundland and elsewhere in the Appalachian Basin. These data also show
617 that the HTD exploration model may be applicable in other post-orogenic extensional
618 basins, with associated drawdown of post-evaporitic brines and magmatic driven
619 hydrothermal fluid flow along extensional faults.

620

621 **Acknowledgements**

622 This project was financed by the PPSC (Pan-Atlantic Petroleum Systems Consortium),
623 PRAC (Petroleum Research Atlantic Canada) and by ISPSG (Irish Shelf Petroleum
624 Studies Group, Ireland). Support from the Earth Science Sector of Natural Resources
625 Canada and by the Department of Natural Resources and Mines of Newfoundland and
626 Labrador is warmly acknowledged. Dr. Ian Knight (Geological Survey of Newfoundland
627 and Labrador) is thanked for assistance during initial fieldwork and samples collection.

628

629

630

631

632 **References**

- 633 Appold MS, Kesler SE & Alt JC (1995) Sulfur isotope and fluid inclusion constraints on
634 the genesis of mississippi valley-type mineralization in the Central Appalachians.
635 *Economic Geology*, **90**, 902-919.
- 636 Al-Aasm IS (2003) Origin and characterization of hydrothermal dolomite in the Western
637 Canada Sedimentary Basin. *Journal of Geochemical Exploration*, **78-79**,9-15.
- 638 Azmy K, Lavoie D, Knight I & Chi G (2008) Dolomitization of the Lower Ordovician
639 Aguathuna Formation carbonates, Port au Port Peninsula, western Newfoundland,
640 Canada: implications for a hydrocarbon reservoir. *Canadian Journal of Earth
641 Sciences*, **45**,795-813.
- 642 Azmy K, Knight I, Lavoie D & Chi G (2009) Origin of dolomites in the Boat Harbour
643 Formation, St. George Group, in western Newfoundland, Canada: implications for
644 porosity development. *Bulletin of Canadian Petroleum Geology*, **57**,81-104.
- 645 Baaker RJ (2003) Package FLUIDs 1. Computer programs for analysis of fluid inclusion
646 data and for modelling bulk fluid properties. *Chemical Geology*, **194**,3-23.
- 647 Banks DA & Yardley BWD (1992) Crush-leach analysis of fluid inclusions in small
648 natural and synthetic samples. *Geochimica et Cosmochimica Acta*, **56**,245-248.
- 649 Banks DA, Boyce AJ & Samson IM (2002) Constraints on the Origins of Fluids Forming
650 Irish Zn-Pb-Ba Deposits: Evidence from the Composition of Fluid Inclusions.
- 651 Boles, JR & Franks, SG (1979). Clay diagenesis in Wilcox Sandstones of southwest
652 Texas: implications of smectite diagenesis on sandstone cementation. *Journal of
653 Sedimentary Research* **49**, 55–70.
- 654 Burden ET, Quinn L, Nowlan GS & Bailey-Nill LA (2002) Palynology and
655 Micropaleontology of the Clam Bank Formation (Lower Devonian) of Western
656 Newfoundland, Canada. *Palynology*, **26**,185-215.
- 657 Carpenter AB (1978) Origin and chemical evolution of brines in sedimentary basins.
658 *Oklahoma Geological Survey Circular*, **79**,60-77.
- 659 Chi G & Ni P (2007) Equations for calculation of NaCl/(NaCl+CaCl₂) ratios and
660 salinities from hydrohalite-melting and ice-melting temperatures in the H₂O-
661 NaCl-CaCl₂ system. *Acta Petrologica Sinica*, **22**.
- 662 Coniglio M, Sherlock R, Williams-Jones AE, Middleton K & Frape SK (1994) Burial and
663 hydrothermal diagenesis of Ordovician carbonates from the Michigan Basin,
664 Ontario, Canada. *Special Publication of the International Association of
665 Sedimentologists*, **21**,231-254.
- 666 Conliffe J, Azmy K, Knight I & Lavoie D (2009) Dolomitization of the Lower
667 Ordovician Watts Bight Formation of the St. George Group, western
668 Newfoundland; evidence of hydrothermal fluid alteration. *Canadian Journal of
669 Earth Sciences*, **46**,247-261.
- 670 Cooper M, Weissenberger J, Knight I, Hostad D, Gillespie D, Williams H, Burden E,
671 Porter-Chaudhry J, Rae D & Clark E (2001) Basin Evolution in Western
672 Newfoundland: New Insights from Hydrocarbon Exploration. *AAPG Bulletin*,
673 **85**,393-418.
- 674 Davies GR & Smith LB, Jr. (2006) Structurally controlled hydrothermal dolomite
675 reservoir facies: An overview. *AAPG Bulletin*, **90**,1641-1690.

- 676 Fontes JC & Matray JM (1993) Geochemistry and origin of formation brines from the
677 Paris Basin, France. *Chemical Geology*, **109**,149-175.
- 678 Friedman GM (2007) Structurally controlled hydrothermal dolomite reservoir facies: An
679 overview: Discussion. *AAPG Bulletin*, **91**,1339-1341.
- 680 Gasparrini M, Bechstaedt T & Boni M (2006) Massive hydrothermal dolomites in the
681 southwestern Cantabrian Zone (Spain) and their relation to the late Variscan
682 evolution. *Marine and Petroleum Geology*, **23**,543-568.
- 683 Gleeson SA & Turner WA (2007) Fluid inclusion constraints on the origin of the brines
684 responsible for Pb-Zn mineralization at Pine Point and coarse non-saddle and
685 saddle dolomite formation in southern Northwest Territories. *Geofluids*, **7**,51-68.
- 686 Goldstein RH & Reynolds TJ (1994) *Systematics of fluid inclusions in diagenetic*
687 *minerals*. Tulsa, SEPM Short Course.
- 688 Goldstein RH (2003) Petrographic analysis of fluid inclusions. In: *Mineralogical*
689 *Association of Canada, Short Course Series* eds Samson I, Anderson A &
690 Marshall D), **32**, 9-53.
- 691 Graser G, Potter J, Koehler J & Markl G (2008) Isotope, major, minor and trace element
692 geochemistry of late magmatic fluids in the peralkaline Ilimaussaq Intrusion,
693 South Greenland. *Lithos*, **106**,207-221.
- 694 Greene M (2008) Multiple generations of dolomitization in the Catoche Formation, Port
695 au Choix, Newfoundland. . In, Memorial University of Newfoundland, **MSc**
696 **Thesis**, 146.
- 697 James NP, Stevens RK, Barnes CR & Knight I (1989) Evolution of a lower Paleozoic
698 continental-margin carbonate platform, northern Canadian Appalachians. *Special*
699 *Publication - Society of Economic Paleontologists and Mineralogists*, **44**,123-
700 146.
- 701 Kesler SE & Pluijm BAvd (1990) Timing of Mississippi Valley-type mineralization:
702 Relation to Appalachian orogenic events. *Geology*, **18**,1115-1118.
- 703 Kesler SE, Appold MS, Martini AM, Walter LM, Huston TJ & Richard Kyle J (1995)
704 Na-Cl-Br systematics of mineralizing brines in Mississippi Valley-type deposits.
705 *Geology*, **23**,641-644.
- 706 Kesler SE, Martini AM, Appold MS, Walter LM, huston TJ & furman FC (1996) Na-Cl-
707 Br systematics of fluid inclusions from Mississippi Valley-type deposits,
708 Appalachian Basin: Constraints on solute origin and migration paths. *Geochimica*
709 *et Cosmochimica Acta*, **60**,225-233.
- 710 Knight I & James NP (1987) The stratigraphy of the Lower Ordovician St. George
711 Group, western Newfoundland; the interaction between eustasy and tectonics.
712 *Canadian Journal of Earth*, **24**,1927-1951.
- 713 Knight I, Azmy K, Greene M & Lavoie D (2007) Lithostratigraphic setting of diagenetic,
714 isotopic, and geochemistry studies of Ibexian and Whiterockian carbonates of the
715 St. George and Table Head groups in western Newfoundland. *Current Research,*
716 *Newfoundland and Labrador Department of Natural Resources*, **Report 07-1**,55-
717 84.
- 718 Knight I, Azmy K, Boyce WD & Lavoie D (2008) Tremadocian carbonate rocks of the
719 lower St. George group, Port au Port peninsula, western Newfoundland:
720 Lithostratigraphic setting of diagenetic, isotopic and geochemical studies. *Current*

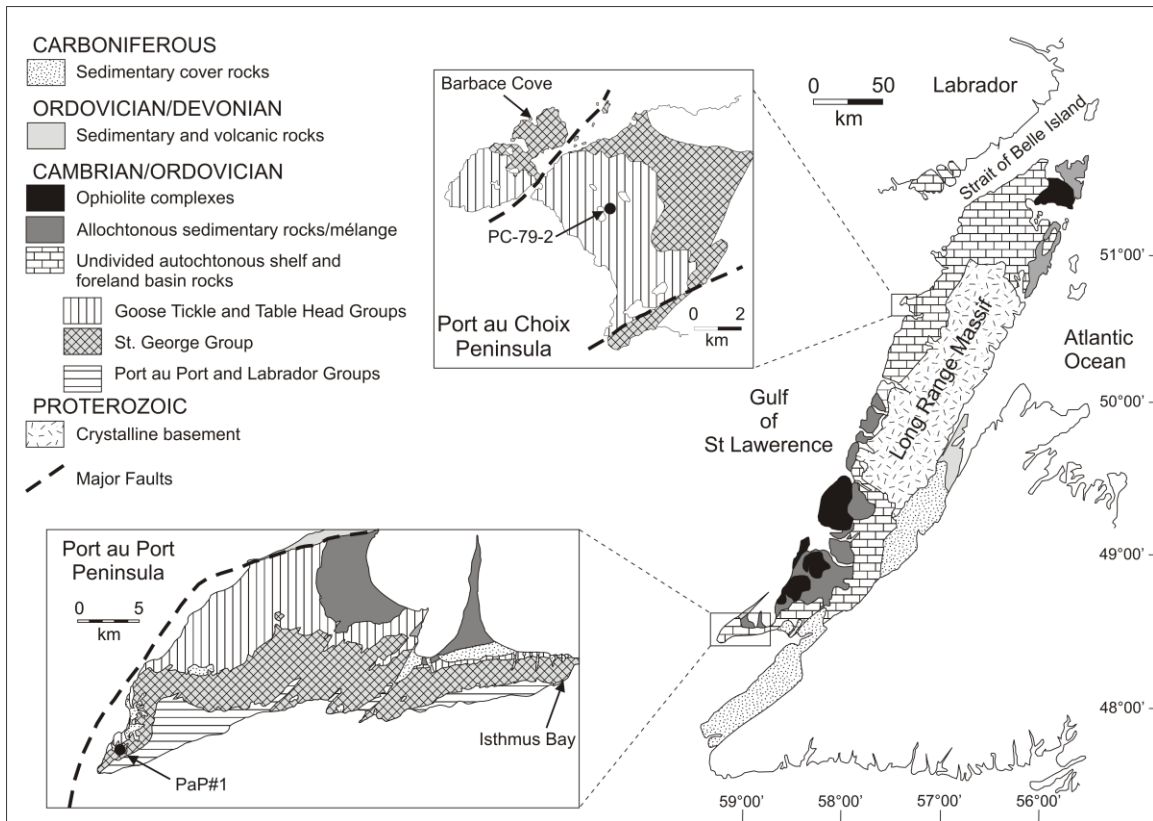
- 721 *Research, Newfoundland and Labrador Department of Natural Resources,*
722 **Report 08-1**,115-149.
- 723 Lane TE (1990) Dolomitization, brecciation, and zinc mineralization and their
724 paragenetic, stratigraphic and structural relationships in the Upper St. George
725 Group (Ordovician) at Daniel's Harbour, western Newfoundland. Ph.D.
726 dissertation, Memorial Univ. Newfoundland.
- 727 Lavoie D & Morin C (2004) Hydrothermal dolomitization in the Lower Silurian Sayabec
728 Formation in northern Gaspé - Matapédia (Quebec): constraint on timing of
729 porosity and regional significance for hydrocarbon reservoirs. *Bulletin of*
730 *Canadian Petroleum Geology*, **52**,256-269.
- 731 Lavoie D, Chi G, Brennan-Alpert P, Desrochers A & Bertrand R (2005) Hydrothermal
732 dolomitization in the Lower Ordovician Romaine Formation of the Anticosti
733 Basin: significance for hydrocarbon exploration. *Bulletin of Canadian Petroleum*
734 *Geology*, **53**,454-471.
- 735 Lavoie D & Chi G (2006) Hydrothermal dolomitization in the Lower Silurian La Vieille
736 Formation in northern New Brunswick: geological context and significance for
737 hydrocarbon exploration. *Bulletin of Canadian Petroleum Geology*, **54**,380-395.
- 738 Lavoie D, Chi G, Urbatsch M & Davis WJ (in press a) Massive dolomitization of a
739 pinnacle reef in the Lower Devonian West Point Formation (Gaspé Peninsula,
740 Québec) – An extreme case of hydrothermal dolomitization through fault-focused
741 circulation of magmatic fluids. *Bulletin of American Association of Petroleum*
742 *Geologists*, v. 94, No. 4.
- 743 Lavoie D, Jackson S & Girard I (in press b) Mg Isotopes in High Temperature Saddle
744 Dolomites from the Lower Paleozoic of Eastern Canada: Significance for the
745 Source of Magnesium and their Origin. In: *American Association of Petroleum*
746 *Geologists, Annual Meeting 2010, Program with abstracts* New Orleans.
- 747 Lavoie D & Chi G (in press) Lower Paleozoic foreland basins in eastern Canada:
748 Tectono-thermal events recorded by faults, fluids and hydrothermal dolomites.
749 *Bulletin of Canadian Petroleum Geology*, **57**, No. 1.
- 750 Lonnee J & Machel HG (2006) Pervasive dolomitization with subsequent hydrothermal
751 alteration in the Clarke Lake gas field, Middle Devonian Slave Point Formation,
752 British Columbia, Canada. *AAPG Bulletin*, **90**,1739-1761.
- 753 Machel HG & Lonnee J (2002) Hydrothermal dolomite--a product of poor definition and
754 imagination. *Sedimentary Geology*, **152**,163-171.
- 755 Machel HG, Lonnee J & Anonymous (2008) Hydrothermal dolomitization; yet another
756 overblown bandwagon? *American Association of Petroleum Geologists, Eastern*
757 *Section Meeting, Pittsburgh, Pennsylvania 2008. Program with abstracts*, p. 41.
- 758 McCaffrey MA, Lazar B & Holland HD (1987) The evaporation path of seawater and the
759 coprecipitation of Br (super -) and K (super +) with halite. *Journal of Sedimentary*
760 *Research*, **57**,928-937.
- 761 Montanez IP & Read JF (1992) Fluid-rock interaction history during stabilization of early
762 dolomites, upper Knox Group (Lower Ordovician), U.S. Appalachians. *Journal of*
763 *Sedimentary Research*, **62**,753-778.
- 764 Nakai Si, Halliday AN, Kesler SE, Jones HD, Kyle JR & Lane TE (1993) Rb-Sr dating of
765 sphalerites from mississippi valley-type (MVT) ore deposits. *Geochimica et*
766 *Cosmochimica Acta*, **57**,417-427.

- 767 Nowlan GS & Barnes CR (1987) Thermal maturation of Paleozoic strata in Eastern
768 Canada from conodont colour alteration index (CAI) data with implications for
769 burial history, tectonic evolution, hotspot tracks and mineral and hydrocarbon
770 exploration. *Bulletin - Geological Survey of Canada*, **367**,47 pp.
- 771 Oakes CS, Bodnar RJ & Simonson JM (1990) The system NaCl---CaCl₂---H₂O: I. The
772 ice liquidus at 1 atm total pressure. *Geochemica et Cosmochimica Acta*, **54**,603-
773 610.
- 774 Pratt BR & James NP (1986) The St George Group (Lower Ordovician) of western
775 Newfoundland; tidal flat island model for carbonate sedimentation in shallow
776 epeiric seas. *Sedimentology*, **33**,313-343.
- 777 Qing H & Mountjoy EW (1994) Formation of coarsely crystalline, hydrothermal
778 dolomite reservoirs in the Presqu'île barrier, Western Canada sedimentary basin.
779 *AAPG Bulletin*, **78**,55-77.
- 780 Rittenhouse G (1967) Bromine in oil-field waters and its use in determining possibilities
781 of origin of these waters. *AAPG Bulletin*, **51**,2430-2440.
- 782 Selleck, B.W., 2006. Hydrothermal alteration of Proterozoic "Grenville" marble and
783 Cambrian Potsdam Group sandstone by seismically-pumped fluids, Adirondack
784 Lowlands of northwestern New York State. *American Association of Petroleum
785 Geologists, Eastern Section 35th Annual Meeting, Buffalo 2006. Program with
786 abstracts*, p. 30.
- 787 Shepherd TJ, Rankin AH & Alderton DHM (1985) *A practical guide to fluid inclusions*,
788 Blackie, London.
- 789 Smith M, Banks DA, Yardley BWD & Boyce AJ (1996) Fluid inclusion and stable
790 isotope constraints on the genesis of the Cligga Head Sn-W deposit, S.W.
791 England. *European Journal of Mineralogy*, **8**,961-974.
- 792 Smith LB, Jr. (2006) Origin and reservoir characteristics of Upper Ordovician Trenton-
793 Black River hydrothermal dolomite reservoirs in New York. *AAPG Bulletin*,
794 **90**,1691-1718.
- 795 Stenzel SR, Knight I & James NP (1990) Carbonate platform to foreland basin; revised
796 stratigraphy of the Table Head Group (Middle Ordovician), western
797 Newfoundland. *Canadian Journal of Earth Sciences*, **27**,14-26.
- 798 Tucker ME & Wright VP (1990) *Carbonate Sedimentology*. Oxford, UK, Blackwell
799 Publishing.
- 800 van Staal CR (2005) North America; Northern Appalachians. In: *Encyclopedia of
801 geology; Volume 4* eds Selley RC, Cocks LRM & Plimer IR) Oxford, Elsevier
802 Academic Press, 81-92.
- 803 Vandeginste V, Swennen R, Gleeson SA, Ellam RM, Osadetz K & Roure F (2009)
804 Thermochemical sulphate reduction in the Upper Devonian Cairn Formation of
805 the Fairholme carbonate complex (south-west Alberta, Canadian Rockies);
806 evidence from fluid inclusions and isotopic data. *Sedimentology*, **56**,439-460.
- 807 Waldron JWF & van Staal CR (2001) Taconian orogeny and the accretion of the
808 Dashwoods block: A peri-Laurentian microcontinent in the Iapetus Ocean.
809 *Geology*, **29**,811-814.
- 810 Walter LM, Stueber AM & Huston TJ (1990) Br-Cl-Na systematics in Illinois basin
811 fluids: Constraints on fluid origin and evolution. *Geology*, **18**,315-318.

- 812 Warren J (2000) Dolomite; occurrence, evolution and economically important
813 associations. *Earth-Science Reviews*, **52**,1-81.
- 814 Wierzbicki R, Dravis JJ, Al-Aasm I & Harland N (2006) Burial dolomitization and
815 dissolution of Upper Jurassic Abenaki platform carbonates, Deep Panuke
816 reservoir, Nova Scotia, Canada. *AAPG Bulletin*, **90**,1843-1861.
- 817 Williams SH, Burden ET & Mukhopadhyay PK (1998) Thermal maturity and burial
818 history of Paleozoic rocks in western Newfoundland. *Canadian Journal of Earth
819 Sciences*, **35**,1307-1322.
- 820 Zhang S & Barnes CR (2004) Arenigian (Early Ordovician) sea level history and the
821 response of shelf and slope conodont communities, western Newfoundland.
822 *Canadian Journal of Earth Sciences*, **41**, 843-865
823

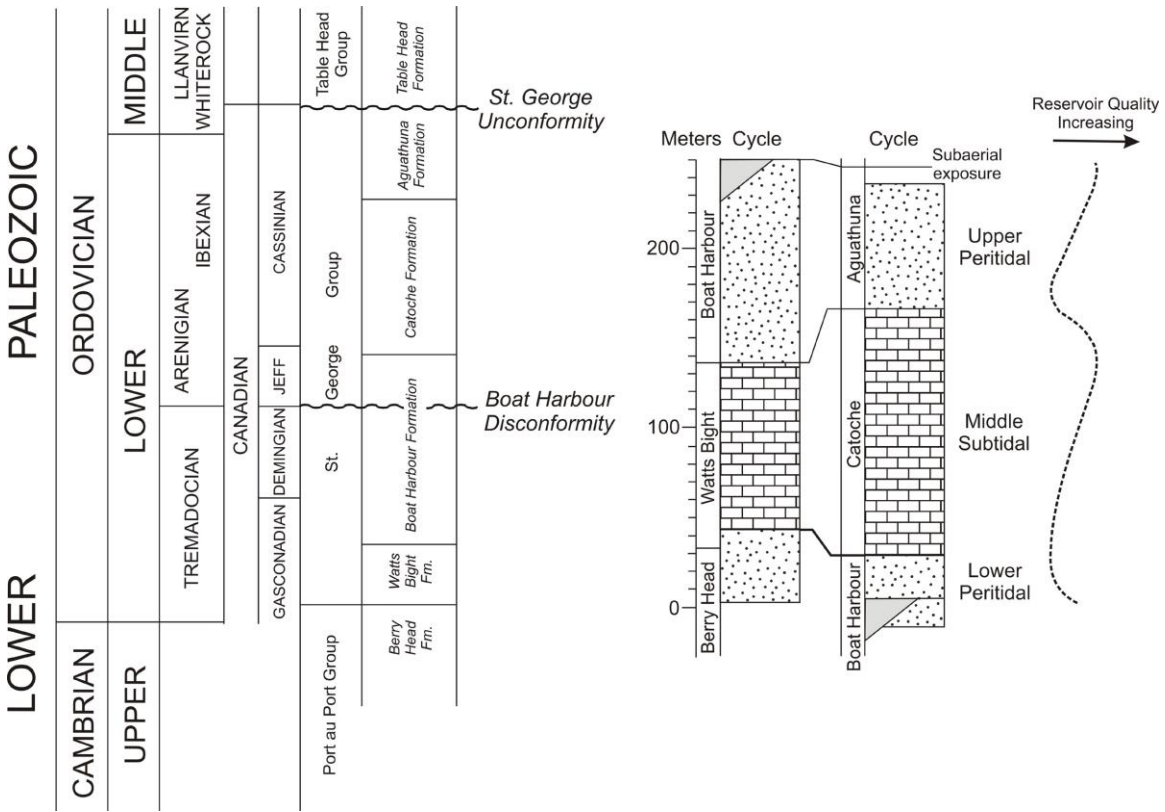
824
825

Figures



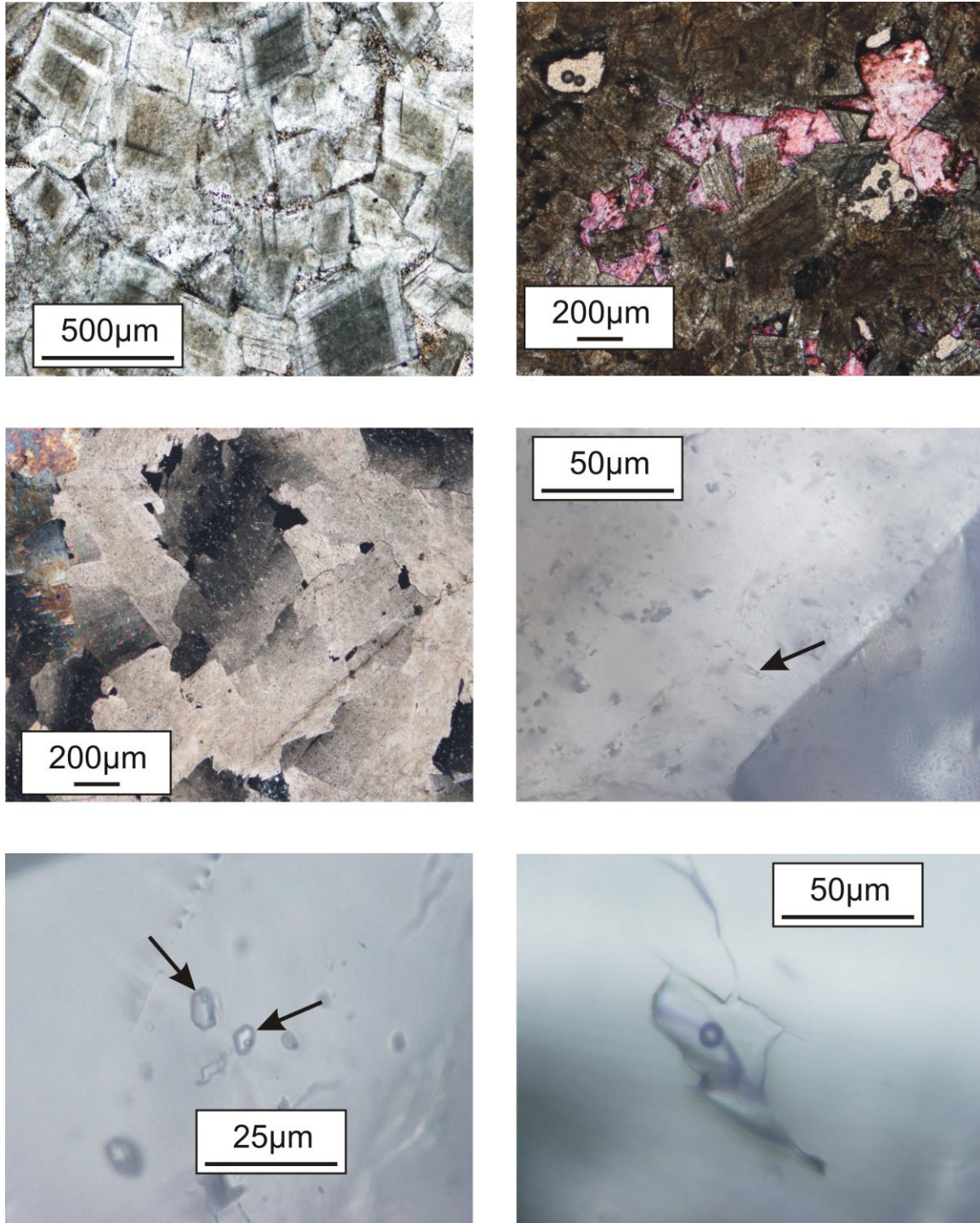
826
827
828
829
830

Figure 1: Simplified map of the geology of Western Newfoundland, with insets showing the geology of the Port au Port and Port aux Choix peninsulas (adapted from Zhang and Barnes, 2004 and Knight et al., 2007)

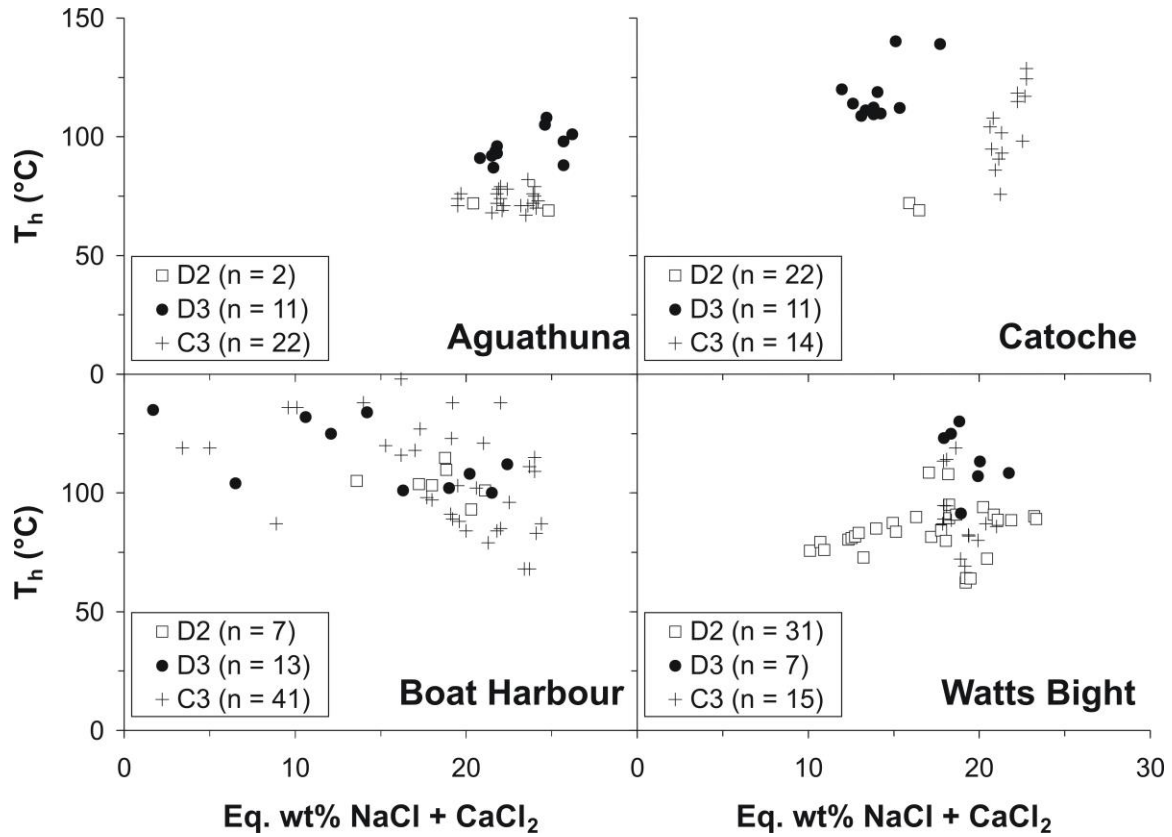


831
832
833
834

Figure 2: Generalized stratigraphic section of the St George Group, including distribution of subtidal and peritidal cycles (from Knight and James, 1987)

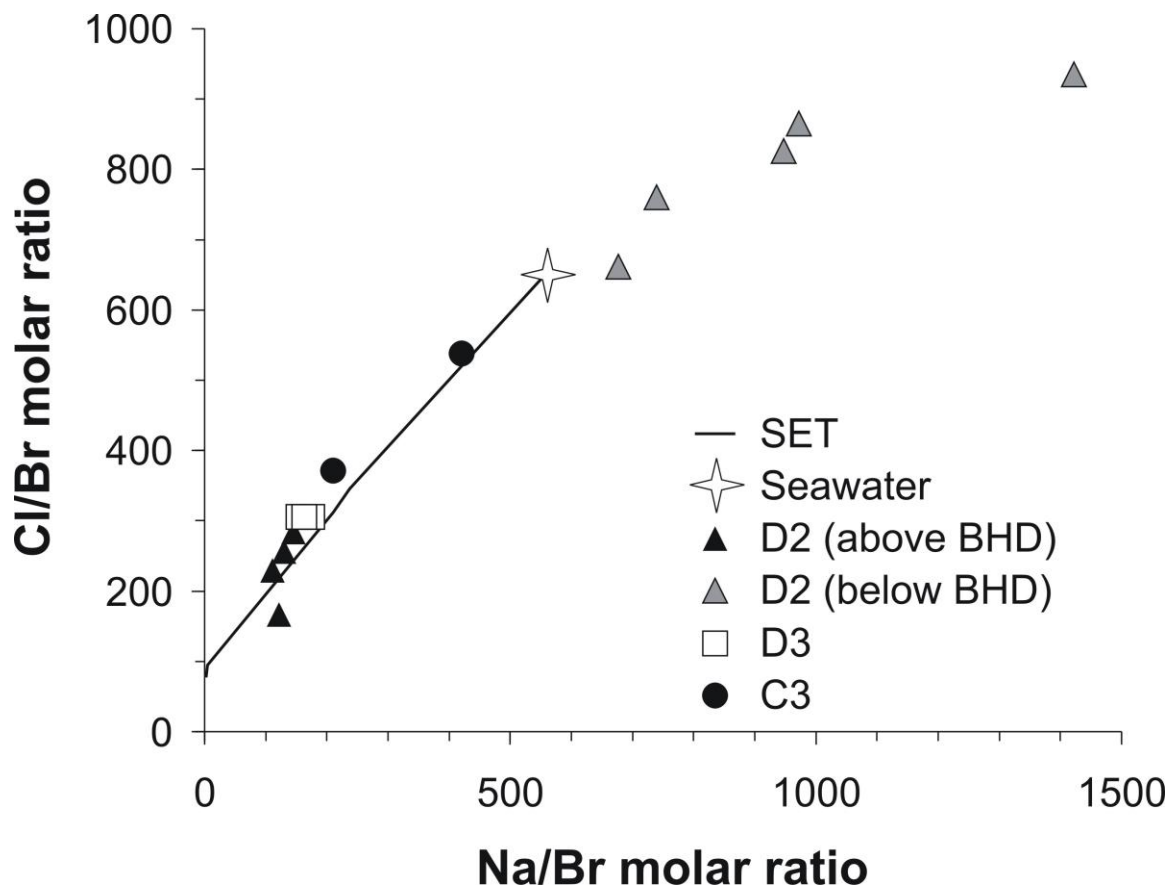


835
 836 **Figure 3:** Photomicrographs from the St. George Group Carbonates. (a) Zoned D2
 837 dolomite rhombs; (b) Stained thin section showing Fe-poor (pink) and Fe-rich (purple)
 838 C3 infilling pores between D2b rhombs; (c) D3 saddle dolomite, showing undulose
 839 extinction; (d) Biphase inclusions in D2 dolomite rhomb. Note inclusion is elongate in
 840 the direction of growth of the dolomite rhomb; (e) Biphase inclusions in D3 dolomite; (f)
 841 Large biphase inclusion in C3 calcite
 842



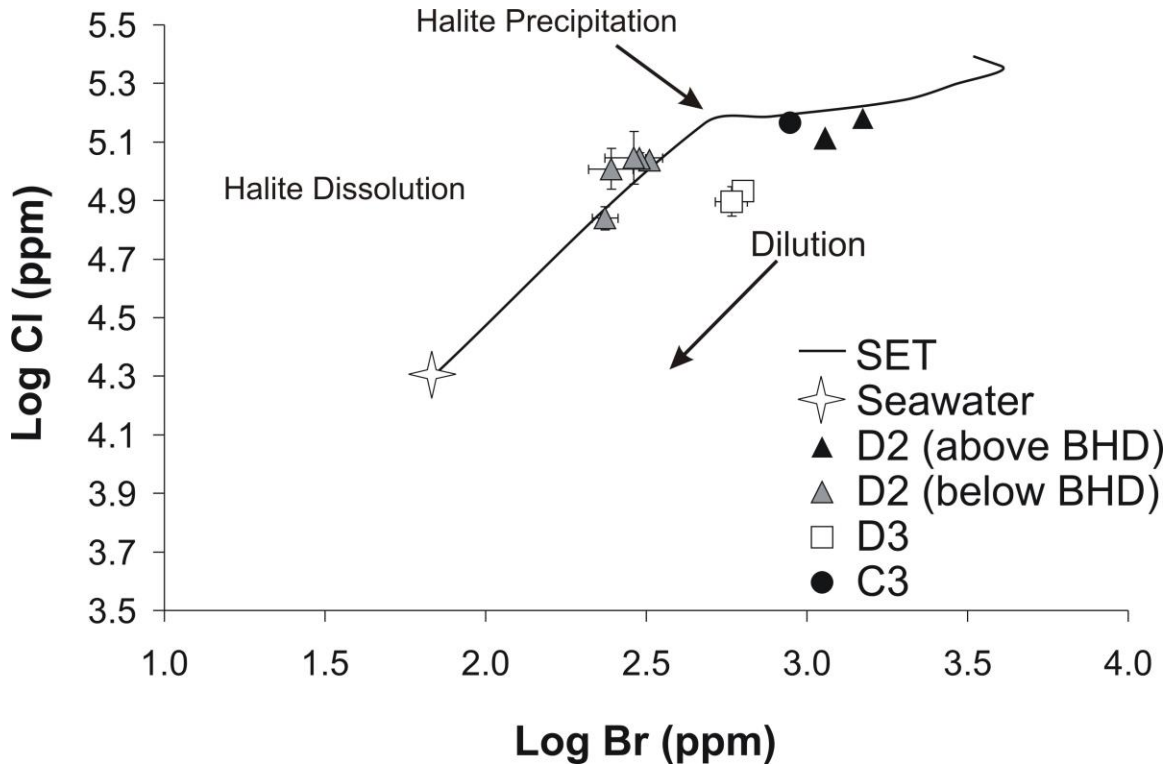
843
844
845
846
847

Figure 4: Bivariate plot of homogenization temperature vs. salinity for fluid inclusions in the D2 and D3 dolomites and C3 calcite of the Aguathuna, Catoche, Boat Harbour and Watts Bight formations



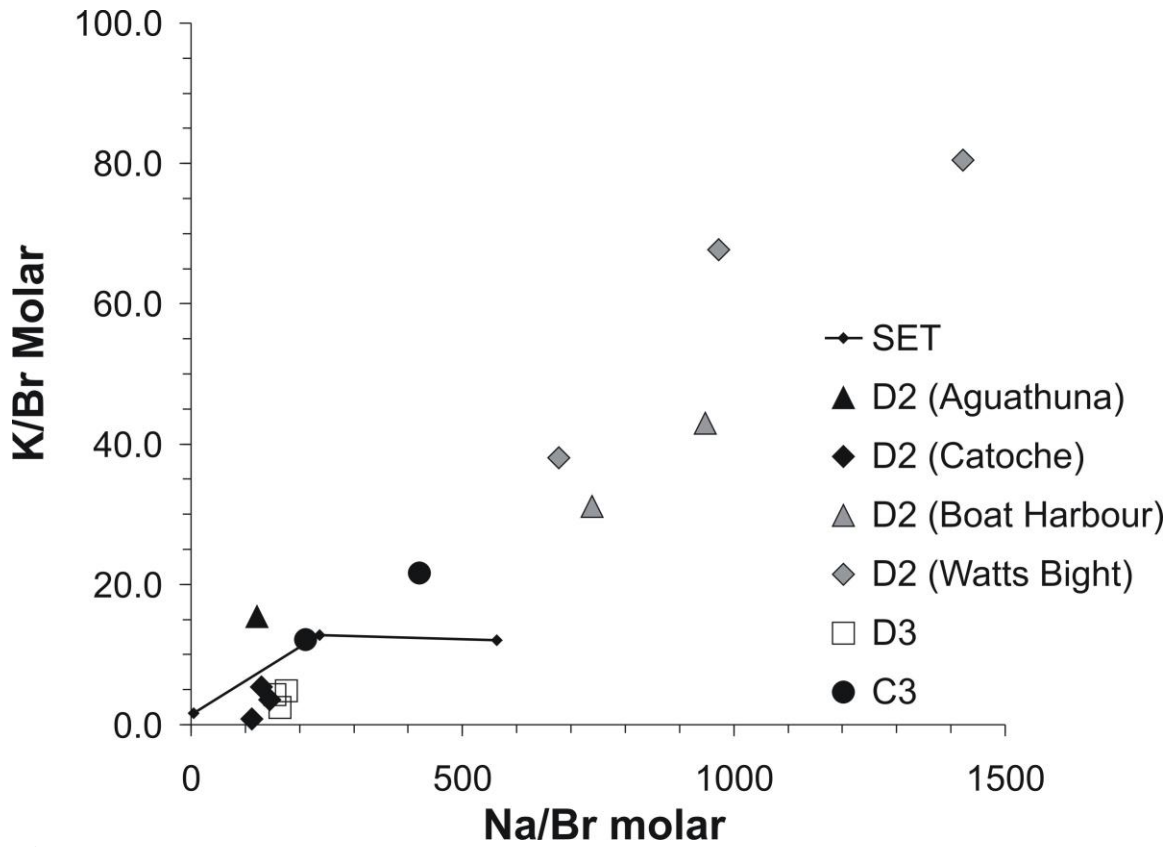
848
849
850
851
852

Figure 5: Na-Cl-Br systematics of the fluid inclusion leachates from St. George Group carbonates. Seawater evaporation trajectory (SET) after McCaffrey et al., 1987. With the exception of D2 samples from below the BHD, samples sit on or close to the SET.



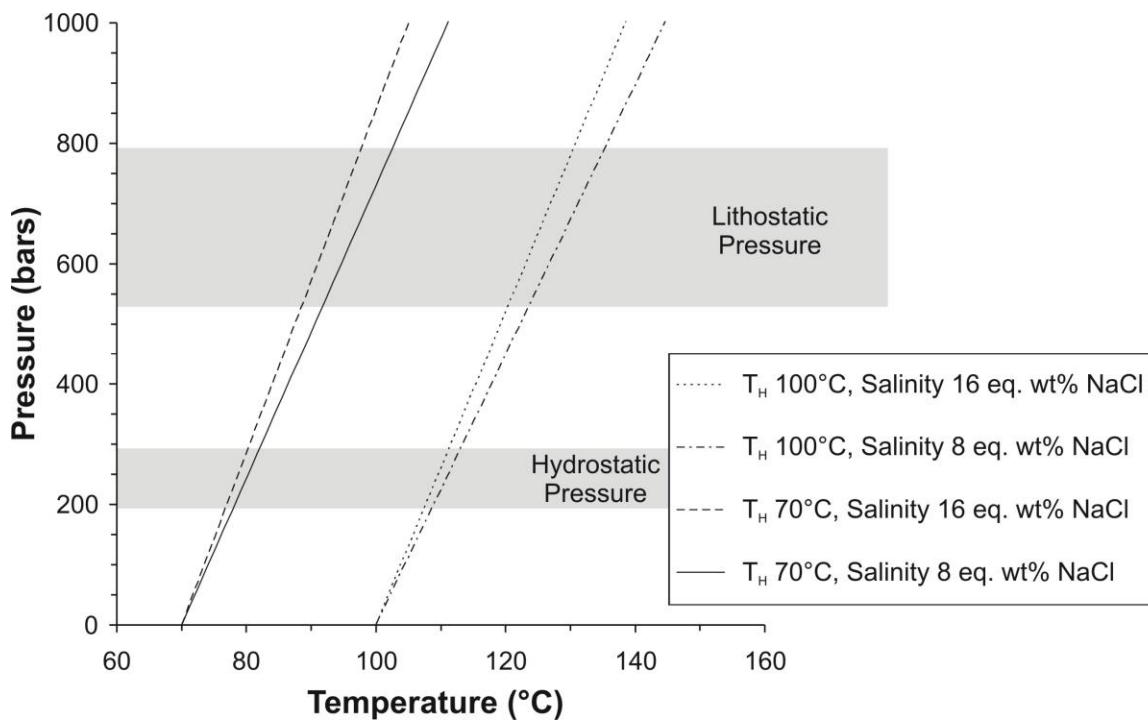
853
854
855
856
857
858

Figure 6: Calculated halogen compositions for D2 (above and below the BHD), D3 and C3 samples. Points are calculated using the mean salinity for each sample, with error bars representing the range of compositions possible using microthermometric data. The data for the Seawater Evaporation Trajectory are from the compilation of Fontes & Matray (1993)



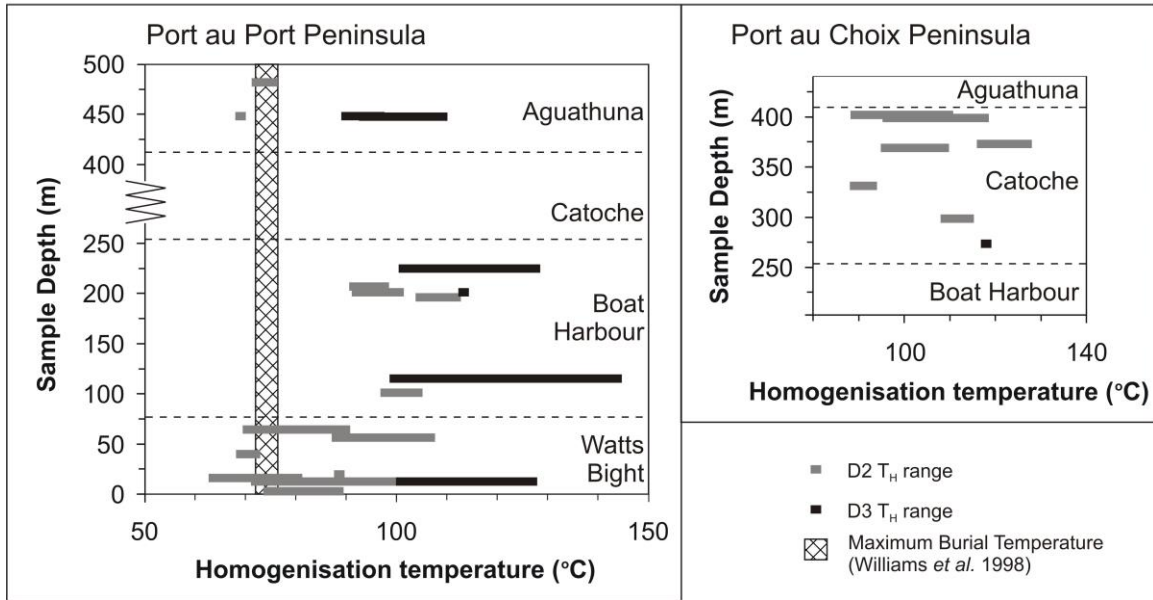
859
860
861
862
863

Figure 7: K-Na-Br systematics of the fluid inclusion leachates from St. George Group carbonates, showing wide variety of K/Br and Na/Br ratios between samples. The data for the SET come from Fontes & Matray (1993)



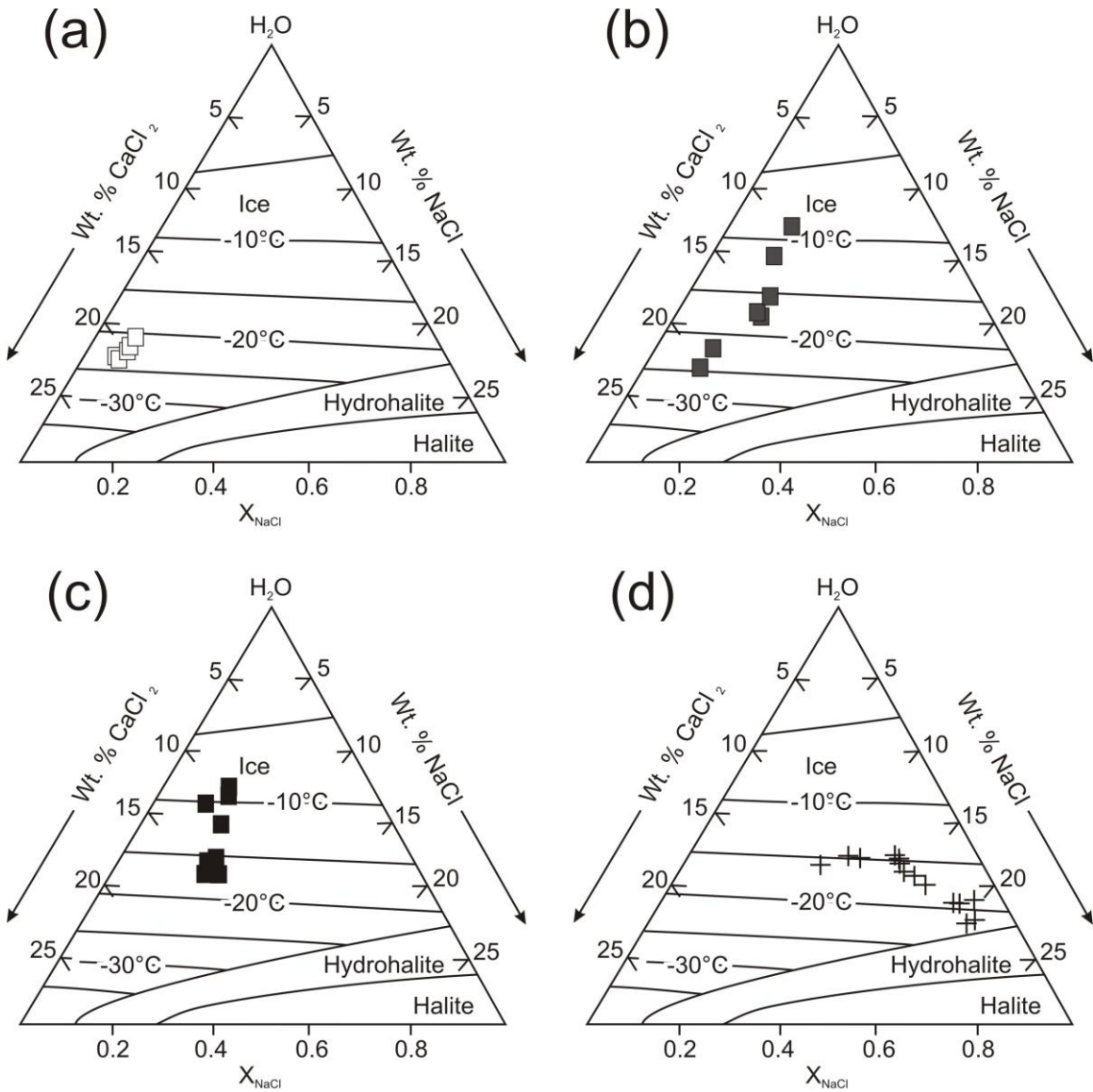
864
865
866
867
868
869

Figure 8: Calculated fluid inclusions isochores for 8 and 16 eq. wt% NaCl fluids trapped at 70 and 100°C. Isochores constructed using the FLUIDS software package (Bakker, 2003). Trapping pressures of 530 to 795 bars for lithostatic pressures and 196 to 294 for hydrostatic pressures calculated using maximum burial depths of 2-3km (Williams et al., 1998)



870
871
872
873
874
875

Figure 9: Fluid-inclusion homogenization temperature for D2 and D3 dolomites vs. maximum burial depth from the Port au Port and Port aux Choix Peninsulas. Maximum burial temperatures indirectly estimated CAI, AAI and GRo (Nowlan and Barnes, 1987; Williams *et al.*, 1998)



876

877 **Figure 10:** Fluid inclusion compositional data (calculated from $T_m(\text{hh})$ and $T_m(\text{ice})$)

878 plotted on the NaCl- CaCl₂-H₂O ternary plot after Oakes et al. (1990) (a) D2 above BHD;

879 (b) D2 below BHD; (c) D3; (d) C3

880

881

882 **Table 1:** Summary of the microthermometric data from D2, D3 and C3 carbonates in the St.
 883 George Group. ¹ Azmy et al. (2008). ² This study. ³ Azmy et al. (2009). ⁴ Conliffe et al.
 884 (2009).

	Sample ID	T _i (°C)	T _m (hydrohalite) (°C)	T _m (ice) (°C)	Salinity (eq. wt% NaCl)	T _h (L) (°C)
Aguathuna¹						
D2	R1-116			-17.4	20.4	69 to 78
D3	R1-147.8	-66 to -53		-31.3 to -17.4	20.4 to 26.2	87 to 101
	R1-148	-62 to -58		-26.2 to -17.4	21 to 24.7	91 to 108
C3	R1-102	-60 to -53		-24.5 to -16.1	19.5 to 24.2	67 to 79
	R1-116	-62 to -50		-24.4 to -20	22.4 to 24.1	64 to 82
Catoche²						
D2	MG401					109 to 114
	MG41	-55.3		-20.7 to -13.6	17 to 21.5	87 to 95
	MG44	-50.1		-15.2 to -12.2	15.9 to 18	85 to 121
	MG13	-84.3 to -75				93 to 122
	MG17	-54.2 to -55	-43.9 to -39.9	-24.8 to -18	19.7 to 23.1	114 to 134
D3	MG108	-54.4 to -51.8	-31 to -30.8	-14.6 to -7.8	12 to 17.7	109 to 140
C3	MG401	-55.2 to 51.2		-24 to 19.7	20.6 to 22.8	72 to 129
Boat Harbour^{2,3}						
D2	BH-35A			-16.4 to -14	17.2 to 18.8	103 to 117
	BH-38A					90 to 102
	BH-42					90 to 99
	BH-A13	-50 to -48		-18.2 to -9.6	13.6 to 21.1	93 to 105
D3	BH-38A	-57 to -52		-20.1 to -8.3	12.2 to 22.4	100 to 134
	BH51-VC			-4.5 to -1	1.7 to 6.5	104 to 135
	BH-A19-2			-10.2 to -7.1	10.6 to 14.2	132 to 134
C3	BH-34			-25.4 to -19.4	22 to 24.4	68 to 87
	BH-35A	-53 to -50		-24 to -14.3	18 to 24	84 to 115
	BH-46	-49		-19.5 to -12.2	16.2 to 22	103 to 182
	BH-51-VC-2	-52 to -49		-20.2 to -5.7	8.9 to 22.5	79 to 123
	BH-A13			-18.1 to -2	3.4 to 21	119 to 138
	BH-A19-2	-57 to -49		-21.2 to -2	3.4 to 22	118 to 168
Watts Bight^{2,4}						
D2	WB-9	-55.2 to -53.8	-31.9	-8.8 to -6.2	10.1 to 12.9	76 to 83
	WB17	-51.4		-15.3 to -13.7	17.1 to 18.2	82 to 109
	WB24			-16 to -9.1	13.2 to 18.6	70 to 95
	WBA2		-39.1 to -38.5	-25 to -22.1	21.9 to 23.3	87 to 90
	WBA4	-54.5 to -51.3	-33.7 to -33.2	-17.4 to -8.4	12.5 to 19.5	62 to 90
	WBA6A					60 to 108
	WBA10A	-55 to -53.1	-33.5 to -32.4	-20.1 to -9.9	14 to 21.8	69 to 94
D3	WBA6A	-52 to -50.2	-31.5 to -30.2	-21.3 to -14.7	17.8 to 21.7	91 to 130
C3	WB-9					99 to 127
	WB17	-55.2 to -52.3		-16.8 to -14.8	17.9 to 19.2	68 to 95
	WB24			-20.1 to -19	20.4 to 21	84 to 87
	WBA2	-51.3 to -51		-18.2 to -17	19.4 to 19.9	80 to 84
	WBA6A	-51.1		-15.6 to -14.7	17.9 to 18.6	114 to 119

886 **Table 2:** Leachate analyses from the St. George Group carbonates. All the data are in
 887 ppm, samples that were analysed but yielded data below the detection limits of the
 888 techniques are indicated by "< detection limit value".

Sample ID	Formation	Mineral	Cl	Br	F	SO₄	Na	K	Li
RI162	Aguathuna	D2	41.10	0.55	0.21	2.89	19.41	4.19	<0.004
MG13	Catoche	D2	438.85	4.31	<0.008	1.44	138.32	1.64	0.02
MG17	Catoche	D2	215.10	1.89	<0.008	2.91	70.95	4.97	0.01
MG33	Catoche	D2	163.50	1.30	<0.008	1.18	54.15	2.24	0.01
BH35	Boat Harbour	D2	47.21	0.13	0.26	1.31	35.06	2.69	0.01
BHA13	Boat Harbour	D2	44.46	0.12	0.10	1.90	32.38	3.82	<0.004
WB9	Watts Bight	D2	56.71	0.19	0.17	1.89	37.63	3.58	0.01
WBA3	Watts Bight	D2	62.61	0.19	0.52	3.80	39.43	2.81	0.02
WBA4	Watts Bight	D2	43.30	0.10	0.27	2.57	42.64	4.09	0.01
RI202	Aguathuna	D3	85.88	0.63	<0.008	0.81	32.03	1.48	<0.004
MG114	Catoche	D3	128.83	0.95	<0.008	1.21	42.09	1.99	<0.004
BHD34.1	Boat Harbour	D3	107.35	0.79	<0.008	1.01	37.22	0.97	<0.004
BH34.2	Boat Harbour	C3	171.91	1.04	<0.008	0.31	63.10	6.18	<0.004
WB20	Watts Bight	C3	40.38	0.17	0.12	1.67	20.42	1.78	<0.004

889

890

891 **Table 3:** Molar ratio data for the minerals sampled from the St. George Group
 892 carbonates. The charge balance calculation is discussed in the text

Sample ID	Formation	Mineral	Charge Balance	Cl/Br (molar)	SO ₄ /Br (molar)	K/Na (molar)	Na/Br (molar)	K/Br (molar)	Li/Na (molar)
RI162	Aguathuna	D2	0.8	167	6.3	0.37	122	15.5	-
MG13	Catoche	D2	0.5	229	0.4	0.02	112	0.8	0.0006
MG17	Catoche	D2	0.5	256	1.8	0.12	130	5.4	0.0004
MG33	Catoche	D2	0.5	284	1.1	0.07	145	3.5	0.0004
BH35	Boat Harbour	D2	1.2	827	12.2	0.13	948	38.0	0.0005
BHA13	Boat Harbour	D2	1.2	865	19.7	0.20	972	31.1	-
WB9	Watts Bight	D2	1.0	661	11.7	0.16	677	42.9	0.0006
WBA3	Watts Bight	D2	1.0	761	24.6	0.12	739	67.7	0.0015
WBA4	Watts Bight	D2	1.5	935	29.6	0.16	1422	80.5	0.0006
RI202	Aguathuna	D3	0.6	305	1.53	0.08	176	4.3	-
MG114	Catoche	D3	0.5	305	1.53	0.08	154	4.8	-
BHD34.1	Boat Harbour	D3	0.5	305	1.53	0.04	163	2.5	-
BH34.2	Boat Harbour	C3	0.6	371	0.4	0.17	210	12.1	-
WB20	Watts Bight	C3	0.8	538	11.9	0.15	420	21.6	-

893

894